GENETIC ANALYSIS OF *BPHSE:* A NOVEL GENE COMPLEMENTING RESISTANCE TO *BORDETELLA PERTUSSIS*-INDUCED HISTAMINE SENSITIZATION

Abbas Raza[1], Sean A. Diehl[2], Laure K. Case[3], Dimitry N. Krementsov[4], Dawei Li[2], Jason Kost[2], Robyn L. Ball[3], Elissa J. Chesler[3], Vivek M. Philip[3], Rui Huang[5], Yan Chen[5], Runlin Ma[5], Anna L. Tyler[3], J. Mathew Mahoney[3,6], Elizabeth P. Blankenhorn[7], and Cory Teuscher[1,8,*]

Departments of Medicine[1], Microbiology and Molecular Genetics[2], Biomedical and Health Sciences[4], Neurological Sciences[6], Pathology and Laboratory Medicine[8], University of Vermont, Burlington, VT, USA 05405

The Jackson Laboratory[3], Bar Harbor, Maine, USA 04609

School of Life Sciences[5], University of the Chinese Academy of Sciences, Beijing, China 100049

Department of Microbiology and Immunology[7], Drexel University College of Medicine, Philadelphia, Pennsylvania, USA 19129

*Address correspondence to: Cory Teuscher, PhD
C331 Given Medical Building
89 Beaumont Avenue
University of Vermont
Burlington, Vermont, 05405, USA
E-mail: c.teuscher@med.uvm.edu

Short title: *Bphse* complements resistance to HA shock

Keywords: histamine, *Bordetella pertussis*, pertussis toxin, anaphylaxis, vascular permeability, shock

Abbreviations: *B*. *pertussis*, *Bordetella pertussis*; Bphs/*Bphs*, *Bordetella pertussis* induced histamine sensitization; *Bphse*, enhancer of *Bordetella pertussis* induced histamine sensitization; Bpss, *Bordetella pertussis* induced serotonin sensitization; Bpbs, *Bordetella pertussis* induced bradykinin sensitization; HA, histamine; Histh/*Histh*, non-*Bordetella pertussis* induced histamine hypersensitivity; *Hrh1*/HRH1, histamine receptor H_1; PTX, pertussis toxin; T1H, type 1 hypersensitivity; VP, vascular permeability; LD, linkage disequilibrium; GPCR, G-protein coupled receptor; ER, endoplasmic reticulum; EMC, endoplasmic membrane protein complex; ERAD, endoplasmic reticulum-associated degradation; MGP, mouse genomes project; MPD mouse phenome database.

ABSTRACT

Histamine is a bioactive amine associated with a plethora of normal and pathophysiological processes, with the latter being dependent on both genetic and environmental factors including infectious agents. Previously, we showed in mice that susceptibility to *Bordetella pertussis* and pertussis toxin (PTX) induced histamine sensitization (Bphs) is controlled by histamine receptor H_1 (*Hrh1*/HRH1) alleles. *Bphs* susceptible and resistant alleles (*Bphs*^{s}/*Bphs*^{r}) encode for two-conserved protein haplotypes. Given the importance of HRH1 signaling in health and disease, we sequenced *Hrh1* across an extended panel of laboratory and wild-derived inbred strains and phenotyped them for Bphs. Unexpectedly, eight strains homozygous for the *Bphs*^{r} allele phenotyped as Bphs^s, suggesting the existence of a modifying locus segregating among the strains capable of complementing Bphs^r. Genetic analyses mapped this modifier locus to mouse chromosome 6; designated *Bphs*-enhancer (*Bphse*), within a functional linkage disequilibrium domain encoding multiple loci controlling responsiveness to histamine (*Bphs*/*Hrh1* and *Histh1-4*). Interval-specific single-nucleotide polymorphism (SNP) based association testing across 50 laboratory and wild-derived inbred mouse strains and functional prioritization analyses resulted in the identification of candidate genes for *Bphse* within a ~5.5 Mb interval (Chr6:111.0-116.4 Mb), including *Atg7, Plxnd1, Tmcc1, Mkrn2, Il17re, Pparg, Lhfpl4, Vgll4, Rho and Syn2*. Taken together, these results demonstrate the power of combining network-based computational methods with the evolutionarily significant diversity of wild-derived inbred mice to identify novel genetic mechanisms controlling susceptibility and resistance to histamine shock.

INTRODUCTION

Histamine (2-[4-imidazole]-ethylamine; HA) is an endogenous biogenic monoamine that is synthesized, stored intracellularly within granules; following cellular activation HA is released by mast cells, basophils, platelets, neurons, and enterochromaffin-like cells in the stomach [1]. After release, free HA mediates its pleiotropic effects by binding to four different seven-transmembrane G-protein-coupled receptors (GPCRs): histamine receptor H_1-H_4 (HRH1, HRH2, HRH3, and HRH4), differentially expressed on target cells in various tissues [2]. HA acting through these receptors influences a diverse array of physiological processes, including brain function, neurotransmission, secretion of pituitary hormones, cell proliferation and differentiation, hematopoiesis, embryonic development, wound healing and regeneration, and the regulation of gastrointestinal, cardiovascular, and secretory functions [2]. In addition, HA plays a major role in inflammation and the regulation of innate and adaptive immune responses in both normal and pathologic states [3, 4].

Historically, HA is most well-known for its role in shock and anaphylaxis [5]. It was first isolated from the parasitic mold ergot of rye (*Claviceps purpurea*) and then synthesized by the decarboxylation of histidine [6-8]. HA was shown to elicit anaphylactic shock-like symptoms when injected into mammals, including bronchiolar constriction, constricted cardiac and pulmonary arteries, and stimulated cardiac contraction [9-11]. Further research firmly established HA as a natural constituent of the body and a mediator of anaphylactic shock [5]. There is significant variability in susceptibility to HA-shock among animal species, with guinea pigs and rabbits being highly susceptible, versus mice and rats which are generally remarkably tolerant to *in vivo* injections of HA [12].

Interestingly, prior exposure to *Bordetella pertussis* (*B. pertussis*) or purified pertussis toxin (PTX) overcomes HA resistance among a subset of laboratory derived inbred strains of mice [13]. This phenotype is designated Bphs for *B. pertussis*-induced HA sensitization [14, 15]. Bphs-susceptible ($Bphs^s$) strains die within 30 minutes following HA injection; which is thought to result from hypotensive and hypovolemic shock while Bphs-resistant ($Bphs^r$) strains remain healthy [16]. The sensitizing activity elicited by exposure to *B. pertussis* is a function of PTX-catalyzed adenosine diphosphate-ribosylation of the alpha subunit of heterotrimeric guanine nucleotide-binding protein ($G\alpha_{i/o}$), specifically $G\alpha_{i1/3}$ [17, 18]. In addition to HA sensitization, PTX-treated mice exhibit increased systemic vascular permeability and sensitization to serotonin (Bpss) and bradykinin (Bpbs) [17, 19].

Our previous genetic studies mapped the autosomal dominant *Bphs* locus controlling susceptibility to mouse chromosome 6 (Chr6) and identified it as histamine receptor H_1 (*Hrh1*/HRH1) [15, 20]. Susceptibility segregates with two conserved *Hrh1*/HRH1 haplotypes, mice with the $Hrh1^s$/$HRH1^s$ allele (encoding Pro^{263}, Val^{312}, Pro^{330}) phenotype as $Bphs^s$ while mice with the $Hrh1^r$/$HRH1^r$ allele (encoding Leu^{263}, Met^{312}, Ser^{330}) are $Bphs^r$. These amino acid changes occur within the third intracellular loop of this G protein-coupled receptor (GPCR): a domain implicated in signal transduction, protein folding, and trafficking. Functionally, $HRH1^s$ and $HRH1^r$ alleles equally activate $G\alpha_{q/11}$, the G protein family members that couple HRH1 signaling to second messenger signaling pathways, indicating that the genetic control of susceptibility and resistance to Bphs is not inherently due to differential activation of either $G\alpha_q$ or $G\alpha_{11}$ [21]. However, the two alleles exhibit differential cell surface expression and altered intracellular trafficking, with the $HRH1^r$ allele selectively retained within the endoplasmic reticulum

(ER). Importantly, all three amino acid residues (Leu^{263}, Met^{312}, Ser^{330}) comprising the HRH1^{r} haplotype are required for altered expression [21].

In this study, we carried out an expanded phenotype screen for Bphs susceptibility and resistance that included previously unstudied wild-derived inbred strains of mice, and identified eight Bphs^{S} strains, despite carrying the Bphs^{R} *Hrh1^{r}*/HRH1^{r} allele. Genetic analyses identified a dominant modifying locus linked to *Bphs*/*Hrh1* capable of complementing *Hrh1^{r}*/HRH1^{r} to create a Bphs^{S} phenotype. We have designated this locus *Bphse* for Bphs-enhancer. Interval-specific single nucleotide polymorphism (SNP) based association testing and functional enrichment is used to identify candidate genes for *Bphse*.

RESULTS

***Hrh1*/HRH1 alleles are highly conserved in mice.** We undertook a genetic approach to screen for evolutionarily selected mechanisms that may be capable of modifying the Bphs^{r} phenotype. Toward this end, we sequenced ~500 bp stretch of genomic DNA encompassing the third intracellular loop of *Hrh1*/HRH1 across 91 laboratory and wild-derived inbred strains of mice (**Table 1**). Surprisingly, other than the three amino acid changes (Pro^{263}, Val^{312}, Pro^{330}→ Leu^{263}, Met^{312}, Ser^{330}) described earlier as "susceptible" (*Hrh1^{s}*/HRH1^{s}) and "resistant" (*Hrh1^{r}*/HRH1^{r}) haplotypes [15], we did not identify any additional non-synonymous amino acid changes. Of the 91 strains, 22 carry the *Hrh1^{r}*/HRH1^{r} allele, whereas 69 carry the *Hrh1^{s}*/HRH1^{s} allele (**Table 1**). We next mapped the evolutionary distribution of the two alleles onto a mouse phylogenetic tree (**Supplementary Figure 1**) [22]. The *Hrh1^{r}*/HRH1^{r} allele was primarily restricted to wild-derived group 7 strains and a select sub-branch of group 1 Bagg albino derivatives, whereas the *Hrh1^{s}*/HRH1^{s} allele was distributed across groups 2-6, which encompasses Swiss mice, Japanese and New Zealand inbred strains, C57/58 strains, Castle mice, C.C. Little DBA and related strains.

Compared to classical inbred strains, wild-derived mice exhibit sequence variation at approximately every 100-200 base pairs and are, in general, more resistant to a variety of pathogens [23-27]. Group 7 strains exemplify this genetic diversity in that it includes representatives of *Mus musculus (M. m) domesticus* (PERA, PERC, WSB, ZALENDE and TIRANO), *M. m. musculus* (PWK, PWD, CZECHI, and CZECHII), *M. m. castaneus* (CAST), *M. m. molossinus* (JF1, MSM, MOLF, MOLD, MOLC), *M. m. hortulanus* (PANCEVO), *M. m. spretus* (SPRET), *M. m. praetextus* (IS), or hybrids of *M. m. musculus*

and *M. m. domesticus* (SKIVE), *M. m. musculus* and *M. m. poschiavinus* (RBF) and of *M. m. castaneus* and *M. m. domesticus* (CALB) [28-30]. This genetic variability represents a rich source of evolutionarily selected diversity and has the potential to lead to the identification of genes controlling novel regulatory features arising from host-pathogen co-evolutionary adaptations.

To screen for functional modifying loci capable of complementing *Hrh1*^{r}/HRH1^{r}, we phenotyped a panel of group 1 (Bagg albino derivatives) and 7 (wild-derived) mice that genotyped as *Hrh1*^{r}/HRH1^{r} for susceptibility to Bphs. While nine *Hrh1*^{r}/HRH1^{r} strains tested were Bphs^{r} as expected, we found eight that were remarkably susceptible to Bphs (**Table 2**). Importantly, these Bphs^{s} strains are confined primarily to group 7 wild-derived strains (**Supplementary Figure 1**) in contrast to *Hrh1*^{r}/HRH1^{r} strains from Group 1 that were mostly Bphs^{r}. Moreover, comparison of the entire *Hrh1* gene (Chr6:114,397,936-114,483,296 bp) between several of the Group 1 and Group 7 phenotyped strains found no segregating non-synonymous structural variants (data not shown) between Bphs^{s} and Bphs^{r} strains suggesting that the complimenting locus/loci in Group 7 is independent of additional previously unidentified *Hrh1*^{s}/HRH1^{s} structural variants.

To confirm the existence of a modifying locus capable of restoring Bphs^{s} in mice with a *Hrh1*^{r}/HRH1^{r} allele and to assess its heritability, we selected a subset of Bphs^{s}-*Hrh1*^{r}/HRH1^{r} (MOLF, PWK) and Bphs^{r}-*Hrh1*^{r}/HRH1^{r} (AKR, CBA, C3H, MRL) strains for follow-up studies. We studied F_1 hybrids between the select strains of interest and HRH1-knockout B6 mice (HRH1KO), which lack a functional *Hrh1*^{s}/HRH1^{s} gene required for Bphs^{s} [31]. These mice can, however, provide potential complementing genetic elements in trans. (B6 × HRH1KO) F_1 and (C3H.*Bphs*^{SJL} × HRH1KO) F_1 harbor the *Hrh1*$^{s/-}$/HRH1$^{s/-}$

allele while (C3H × HRH1KO) F_1, (CBA × HRH1KO) F_1, (MRL × HRH1KO) F_1 and (AKR × HRH1KO) F_1 have the *Hrh1*$^{r/-}$/HRH1$^{r/-}$ allele. Both *Hrh1*^{s}-by-HRH1KO F_1 hybrids were Bphs^{s}, whereas the *Hrh1*^{r}-by-HRH1KO F_1 hybrids were Bphs^{r} (**Table 3**), in agreement with our prior finding that *Hrh1*$^{s/-}$/HRH1$^{s/-}$ controls dominant susceptibility to Bphs [14]. In contrast, (MOLF × HRH1KO) F_1 and (PWK × HRH1KO) F_1 hybrids, that harbor the *Hrh1*$^{r/-}$/HRH1$^{r/-}$ allele, were Bphs^{s}. This data supports the existence of one or more dominant loci in MOLF and PWK capable of complementing Bphs^{r} in *Hrh1*$^{r/-}$/HRH1$^{r/-}$ mice.

A functional linkage disequilibrium (LD) domain on Chr6 encodes multiple loci controlling HA-shock. Given the evidence from inbred strains of mice indicating that a quarter or more of the mammalian genome consists of chromosomal regions containing clusters of functionally related genes, i.e., functional linkage disequilibrium (LD) domains [32, 33], we hypothesized that the dominant locus complementing *Hrh1*^{r}/HRH1^{r} may reside within such a LD domain. Support for the existence of a functional LD domain controlling responsiveness to HA is supported by our recent finding that *Histh1-4*, four QTL on Chr6:45.9-127.9 Mb controlling age- and inflammation-dependent susceptibility to HA-shock in SJL/J, FVB/NJ, NU/J, and SWR/J mice, are in strong LD with *Bphs*/*Hrh1 (*Chr6:114,397,936-114,483,296 bp) [34, 35].

To test this, we generated 114 (MOLF × HRH1KO) × HRH1KO backcross (BC) mice (**Table 3**), genotyped their *Hrh1* alleles, and phenotyped them for Bphs. As expected, none of the 54 homozygous HRH1KO mice phenotyped as Bphs^{s}. Of the 114 BC mice studied, 54 (47%) were Bphs^{s}, which is consistent with genetic control by a single locus. Furthermore, of the 60 HRH1^{MOLF} (*Hrh1*^{r}/HRH1^{r}) mice, 54 were Bphs^{s} and 6

were Bphs^r, indicating that the locus capable of complementing Bphs^r is in fact linked to *Bphs*/*Hrh1*. We have designated this locus *Bphse* for Bphs-enhancer.

To further test the hypothesis that *Bphse* is linked to *Hrh1*, we generated a cohort of Bphs-phenotyped (AKR × PWK) × AKR BC1 mice and performed linkage analysis using informative markers across a ~70 Mb region encompassing *Hrh1*. Both AKR and PWK mice carry the *Hrh1^r*/HRH1^r allele; however, unlike AKR mice, which are Bphs^r, PWK mice are Bphs^s (**Table 2**). Overall, 83 of 168 (49%) (AKR × PWK) × AKR BC1 mice were Bphs^s (**Table 4**). This is in agreement with the segregation of *Bphse* in (MOLF × HRH1KO) × HRH1KO BC1 mice and provides further evidence that *Bphse* is in LD with *Bphs*/*Hrh1*. Marker loci from *rs36385580* thru *D6MiT135* (Chr6: 59.3-128.8 Mb) exhibited significant linkage to Bphs^s with maximal linkage across the interval bounded by *D6MiT102* (Chr6:93,463,949-93,464,093 bp) and *rs31698248* (Chr6:120,207,213 bp) encompassing *Hrh1* (Chr6:114,397,936-114,483,296 bp).

We next confirmed the existence and physical location of *Bphse* by congenic mapping. Marker-assisted selection was used to introgress the *Bphse^{MOLF}* and *Bphse^{PWK}* intervals onto the Bphs^r C3H and AKR backgrounds, respectively. Starting at N5 through N10, heterozygous and homozygous BC mice were phenotyped for Bphs (**Figure 1**). Compared to C3H (C3H and C3H.*Bphse$^{C3H/C3H}$*) and AKR (AKR and AKR.*Bphse$^{AKR/AKR}$*) mice, both C3H.*Bphse$^{C3H/MOLF}$* and AKR.*Bphse$^{AKR/PWK}$* mice were Bphs^s. Overall, *Bphse$^{C3H/MOLF}$* and *Bphse$^{AKR/PWK}$* mice were significantly more susceptible to Bphs than *Bphse$^{C3H/C3H}$* and *Bphse$^{AKR/AKR}$* mice ($\chi^2 = 60.63$, df = 1, $p<0.0001$). The physical mapping results confirm the linkage of *Bphse* to *Bphs*/*Hrh1* and *Histh1-4* (Chr6:45.9-127.9 Mb) [34, 35], and importantly provide strong support for the existence of a functional LD domain

on Chr6 encoding multiple loci controlling susceptibility to HA-shock following exposure to environmental factors and infectious agents, including influenza A [35].

Identification of candidate genes for *Bphse.* Given that many laboratory and few wild-derived inbred strains have undergone deep sequencing (30–60× genome coverage) with publicly available variant datasets in Mouse Phenome Database (MPD; https://phenome.jax.org/) [36] and Mouse Genomes Project (MGP; https://www.sanger.ac.uk/data/mouse-genomes-project/) [37], we retrieved all coding and non-coding single nucleotide polymorphism (SNP) data available across the *Bphse* congenic interval (Chr6:59.3-128.8 Mb) among our seventeen Bphs phenotyped *Hrh1*^{r}/HRH1^{r} mouse strains (**Table 2**). As expected, this dataset lacked SNP coverage for several of the wild-derived inbred strains (>98% SNP missing compared with C57BL/6J) that were phenotyped for Bphs in this study. To complement our dataset, we utilized Chr6 region capture sequencing (see Materials and Methods) to sequence and identify SNPs within the *Bphse* interval, and integrated these SNPs with the publicly available dataset. This approach yielded a total of 1,303,072 SNPs among which 13,257 SNPs had 100% coverage (no missing genotypes) across all seventeen strains.

To identify variants that segregate with Bphs^{s} among *Hrh1*^{r}/HRH1^{r} strains, we used efficient mixed-model association (EMMA) [38] and both the larger dataset of 1,303,072 SNPs as well as the smaller dataset of 13,257 SNP with the anticipation that having complete genotypes would increase the power to detect segregating variants. However, both datasets yielded no significant or suggestive associations (data not shown) which led us to speculate that perhaps the number of mouse strains available for genetic association analysis may be a limiting factor. To test this, we asked if we could identify

genetic variants that segregate with Bphs^{s} independent of *Hrh1*/HRH1 haplotype with the rationale that this approach will identify *Bphs*/*Hrh1* (positive control) as well as polymorphic gene candidates for *Bphse*. Moreover, *Bphse* expressivity requires *Hrh1*/HRH1. This method greatly enhanced the number of mouse strains for genetic association analysis, as numerous mouse strains have been phenotyped for Bphs over the years by us and others [15, 17, 19, 39, 40].

To accomplish this, we generated SNP datasets as before but across a larger panel of 50 inbred mouse strains (*Hrh1*^{r}/HRH1^{r} and *Hrh1*^{s}/HRH1^{s}) (**Supplementary Table 1**). Using this approach, we identified 3 SNPs in *Atg7* as significant with a stringent cut-off (*p<3.81E-06*) and another 163 SNPs in 27 genes with a moderate cut-off (*p<5.00E-02*) that were associated with Bphs^{s} (**Figure 2A** and **Supplementary Table 2**). There was no difference in predicted candidate genes using either the smaller dataset (13,257 SNPs) or the larger dataset (1,303,072 SNPs). It is important to reiterate that this approach of combining both *Hrh1*^{r}/HRH1^{r} and *Hrh1*^{s}/HRH1^{s} mouse strains may predict candidates for both *Bphs* and *Bphse*. Thus, *Hrh1,* which is a positive control for this analysis and whose polymorphism has been earlier shown to underlie *Bphs* among laboratory inbred strains [15], was among the candidate genes supporting the predictions from this analysis. We also know that the DNA sequence of the entire *Hrh1* gene (~85 kb) among several *Hrh1*^{r}/HRH1^{r} strains harbor no additional segregating nonsynonymous structural variants (data not shown) between Bphs^{s} and Bphs^{r} mice, excluding involvement of any previously unidentified *Hrh1*/HRH1 structural alleles underlying *Bphse*.

The *Bphse* predicted candidate genes cluster in a narrow interval of ~5.5 Mb on Chr6:111.0-116.4 Mb (**Figure 2A**). Given that our larger dataset (1,303,072 SNPs) includes several thousand SNPs in this shortlisted region of ~5.5Mb, we asked if we could impute the missing SNPs and do a high-dimensional association run. To impute missing SNPs, we utilized the Viterbi algorithm implemented in HaploQA [41, 42] and generated a complete dataset of 78,334 SNPs across Chr6:111.0-116.4 Mb. Using this, we ran a high-resolution genetic association analysis and found *Atg7*, *Tmcc1, Il17re*, *Vgll4*, and several others as top hits for *Bphse* (*p<5.00E-02*) (**Figure 2B-C**; **Supplementary Table 3**).

As a complementary approach to identify positional candidates for *Bphse*, we employed machine-learning computation, using functional genomic networks [43] to identify network-based signatures of biological association. To this end, we used prior knowledge to generate a list of Bphs-associated biological processes and retrieved gene sets functionally associated with each term. The terms and their justifications are as follows:

- *Type I hypersensitivity/anaphylaxis*: The death response following systemic HA challenge exhibits symptoms of type I hypersensitivity/anaphylaxis including respiratory distress, vasodilation, and anaphylactic shock [44].
- *Cardiac*: There is evidence suggesting that anaphylactic shock in mice is caused by decreased cardiac output, rather than systemic vasodilation [45].
- *Histamine*: Bphs is induced by a systemic HA challenge [15].
- *G-protein coupled receptor*: HRH1 signaling is required for the Bphs phenotype, and all HA receptors belong to the family of G-protein coupled receptors [46].

- *Pertussis toxin*: Bphs is induced in mouse strains by PTX [12].
- *Vascular permeability* (VP): Hypersensitivity to HA exhibits vascular leakage in skin and muscles [34, 35].
- *Endoplasmic reticulum (ER)/endoplasmic membrane protein complex (EMC), and endoplasmic reticulum-associated degradation (ERAD)*: The two HRH1 alleles exhibit differential protein trafficking and cell surface expression with the $HRH1^{r}$ allele primarily retained in the ER [21]. The EMC and ERAD are intimately involved in regulating GPCR translocation to the plasma membrane [47, 48].

Each of the seven gene sets define a putative Bphs-related process that forms a distinct subnetwork of the full functional genomic network. Using this approach, we identified several hundred genes within the *Bphse* congenic locus that are functionally associated with each biological process, and thus could be gene candidates (**Supplementary Table 4**).

Genes that are predicted to be highly functionally related to a trait may not have functional variant alleles segregating in the study population, and may therefore be unlikely to drive the observed strain differences in $Bphs^{s}$. Using the list of polymorphic genes identified through high-resolution genetic association testing (**Figure 2**), we normalized and plotted the respective genetic association score ($-\log_{10} p_{EMMA}$) with functional enrichment ($-\log_{10} FPR$) to focus on genes that overlap both approaches (**Figure 3A**). The final ranking was calculated by defining a final gene score (S_{cg}) for each gene, which is the sum of the (normalized) $-\log_{10}(FPR)$ and the $-\log_{10}(p_{EMMA})$ (**Figure 3B**). The top ten candidates for *Bphse* as ranked using S_{cg} are: *Atg7, Plxnd1, Tmcc1, Mkrn2, Il17re, Pparg, Lhfpl4, Vgll4, Rho and Syn2.* It is interesting to note that the predicted

candidates for *Bphse* not only overlap *Bphs*/*Hrh1* but two additional QTLs, *Histh3* (Chr6:99.5-112.3 Mb) and *Histh4* (Chr6:112.3-127.9 Mb), controlling age- and inflammation-dependent susceptibility to HA shock in SJL/J, FVB/NJ, NU/J, and SWR/J mice [34, 35]. Importantly, our findings support the existence of a smaller functional LD domain on Chr6:111.0-116.4 Mb (~5.5 Mb interval) that controls susceptibility to HA-shock elicited by both PTX dependent and independent mechanisms (**Supplementary Figure 2**).

DISCUSSION

B. pertussis and PTX elicit *in vivo* a variety of immunologic and inflammatory responses, including systemic vascular hypersensitivity to serotonin (Bpss), bradykinin (Bpbs), and HA (Bphs) [17]. Utilizing classical laboratory derived inbred strains of mice, we and others showed that susceptibility to Bpss, Bpbs, and Bphs are under unique genetic control with Bpss^{s} and Bpbs^{s} being recessive traits [17, 19] and Bphs controlled by the single autosomal dominant locus *Bphs* [14, 49], which we subsequently identified at *Hrh1*/HRH1 [15]. Herein, we present data from several wild-derived inbred strains of mice that harbor the *Hrh1^{r}*/HRH1^{r} allele which nevertheless phenotype as Bphs^{s}. This is suggestive of the existence of an evolutionarily selected modifying locus that can complement *Hrh1^{r}*/HRH1^{r} and is supported by the unique phylogenetic distribution of such strains (**Supplementary Figure 1**).

Our results with the genetic cross [(MOLF x C3H) x C3H BC mice] confirm the existence of a dominant modifying locus (*Bphse*) capable of complementing Bphs^{s} in mice with an *Hrh1^{r}*/HRH1^{r} allele. We also found that *Bphse* requires *Hrh1*/HRH1, as no BC1 mice that genotype as *Hrh1$^{-/-}$* were Bphs^{s} (**Table 3**). Among BC1 mice that genotype as *Hrh1$^{MOLF/-}$*, 10% of mice phenotyped as Bphs^{r} indicating that *Bphse* is in LD with *Bphs*/*Hrh1*. Linkage scans using microsatellite markers validated significant linkages to Chr6, with maximal significance around *Bphs*/*Hrh1* (**Table 4**). In addition, we mapped the physical location of this locus by making congenic mice (C3H.*Bphse*$^{MOLF+/-}$ and AKR.*Bphse*$^{PWK+/-}$) that captured the *Bphse* locus on Chr6 (59.3-128.8 Mb, **Figure 1**) and replicated the phenotype. To our knowledge, this is the first study assessing Bphs^{s} in

multiple wild-derived inbred strains of mice, and clearly establish their utility in identifying novel genetic mechanisms controlling HA-shock.

Aside from genetics, several factors could influence HA sensitivity after exposure to *B. pertussis* and PTX including age, sex, and route of sensitization/challenge [12]. In our phenotyping experiments, we used 8-12-week-old mice of each sex and did not find any sex differences. This agrees with earlier studies that found no sex differences in Bphs^{s} [47]. We also tested the route of administration of PTX and HA challenge using the intraperitoneal and intravenous routes and found no difference (data not shown). We have not tested the effect of age on Bphs^{s} amongst the various strains; however, work from Munoz and others have reported a significant effect of age [12]. It is possible that some of the strains that are Bphs^{r} will exhibit Histh^{s} as they age or following treatment with complete Freund's adjuvant [34, 35].

The region encoding *Bphse* is very large and contains hundreds of genes (Chr6:59.3-128.8 Mb). Until recently, interval specific recombinant congenic mapping was the gold standard to delimit large QTLs associated with a phenotype [48]. Of the thousands of QTLs for various phenotypes and diseases, only a small fraction of genes have been identified through sub-congenic mapping, phenotyping and sequencing. The identification of candidate genes from large genomic regions has been revolutionized with the advent of advanced sequencing technologies and genome wide association studies (GWAS) [50]. For example, the Sanger Institute has sequenced 16 inbred laboratory and wild-derived mouse genomes and The Jackson Laboratory, in conjunction with the University of North Carolina, has genotyped several hundred laboratory inbred strains using the Mouse Diversity Array, that altogether provides an almost complete picture of

genetic variation among the various strains. Our approach, however, is different from other mouse GWAS studies that have been done to identify candidate loci for several diseases [51]. Instead of running a full genome scan across a large panel of Bphs phenotyped strains, we tested association of susceptibility exclusively across the *Bphse* locus (Chr6:59.3-128.8 Mb). This allowed us to use the information gathered from the genetic cross and congenic mapping and delimit the region to be screened for association.

Our first screen using genotype and phenotype data across seventeen *Hrh1*^{r}/HRH1^{r} mouse strains did not yield any significant hits, due to limitation in the number of strains used. To overcome this problem, we excluded *Hrh1* genotype as a co-variate. Given that several dozen laboratory inbred mouse strains (Group 2, 3 and 4) have been phenotyped for Bphs [15, 17, 19, 39, 40] and also to circumvent the sample size limitation in genetic association testing, we searched for genetic polymorphism across the 50 mouse strains that could explain overall Bphs^{s}. *Hrh1,* which is our positive control and associated with Bphs^{s} among classical laboratory inbred strains [15], was identified as a significant hit supporting the validity of this approach. The use of imputed datasets across 50 phenotyped strains further refined the SNPs associated with Bphs^{s} (**Figure 2**).

Recently, a quantitative trait gene prediction tool has been described that utilizes functional genomics information (gene co-expression, protein-protein binding data, ontology annotation and other functional data) to rank candidate genes within large QTLs associated with a respective phenotype [43]. This methodology uses biological prior knowledge to predict candidate genes that could influence multiple pathways affecting the phenotype. We utilized this approach for Bphs, which is known to involve cardiac,

vascular, and anaphylactic mechanisms [44, 45]. Because the selection of phenotype-associated gene sets is critical for final gene predictions, several terms were used to incorporate sub-phenotypes equivalent to Bphs in the expectation that use of multiple terms would help identify candidate loci for *Bphse*. Integration of functional predictions with genetic association (S_{cg}, **Figure 3**) allowed us to focus on only those candidates that reached significance in both approaches.

Given that there is differential cell surface expression of HRH1 depending on the haplotype, it is tempting to speculate that *Bphse* may aid in the folding, trafficking and/or surface delivery of HRH1 [51, 52]. In this regard, *Tmcc1* (transmembrane and coiled-coil domain family 1) and *Atg7* (autophagy related 7) are promising candidates because of their known roles in protein trafficking in cells. *Tmcc1* is an ER membrane protein that regulates endosome fission and subsequent cargo trafficking to the Golgi [53]. Similarly, *Atg7* is implicated in translocation of cystic fibrosis transmembrane conductance regulator (CFTR) to the surface [54]. CFTR is a multi-pass membrane GPCRs like HRH1 in that both protein classes pass several time through the cell membrane, thus it is tempting to suggest *Atg7* may act in a similar fashion to translocate HRH1 to the surface thereby resulting in the $Bphs^s$ phenotype. It will be interesting to test the surface expression of HRH1 among the $Hrh1^r$/$HRH1^r$ strains that phenotype as $Bphs^s$ (**Table 2**). Results using bone marrow chimeras suggest that $Bphs^s$ is a function of the non-hematopoietic compartments [48], so several cell types (endothelial, epithelial, stromal cells) are potential candidates for this cell surface expression analysis.

In addition to *Tmcc1* and *Atg7*, several other predicted candidates for *Bphse* may have potential relevance to phenotypes associated with Bphs including anaphylaxis and

mast cell degranulation, and cardiovascular effects (**Supplementary Table 4**). Proliferator-activated receptor-gamma (*Pparg)* encodes a nuclear receptor protein belonging to the peroxisome proliferator-activated receptor (Ppar) family. Activation of PPARγ suppresses mast cell maturation and is involved in allergic disease [55, 56]. Because mast cells are major drivers of pathological events in anaphylaxis [57], *Pparg* may be highly relevant to Bphs. In addition, increased PPARγ expression is associated with cardiac dysfunction [57]. It will be interesting to quantify the mRNA expression of some of these candidates between $Bphs^s$ and $Bphs^r$ strains and investigate whether they interact with HRH1.

Importantly, the fact that *Bphse* resides within a smaller functional LD that includes *Histh3* and *Histh4* (**Supplementary Figure 2**) is of potential clinical significance. *Histh* is an autosomal recessive genetic locus that controls susceptibility to *B. pertussis* and PTX-independent, age- and inflammation-dependent HA-shock in SJL/J mice [34, 35]. Four sub-QTLs (*Histh1-4*) define *Histh*, each contributing 17%, 19%, 14%, and 10%, respectively, to the overall penetrance of Histh. Importantly, *Histh* is syntenic to the genomic locus most strongly associated with systemic capillary leak syndrome (SCLS) in humans (3p25.3). SCLS or Clarkson disease is a rare disease of unknown etiology characterized by recurrent episodes of vascular leakage of proteins and fluids into peripheral tissues, resulting in whole-body edema and hypotensive shock. Additionally, $Histh^s$ SJL/J mice recapitulate many of the cardinal features of SCLS, including susceptibility to HA- and infection-triggered vascular leak and the clinical diagnostic triad of hypotension, elevated hematocrit, and hypoalbuminemia and as such makes them a natural occurring animal model for SCLS [34, 35]. Clearly, detailed genetic analysis and

identification of the causative genes underlying *Bphse*, *Histh3*, and *Histh4* may reveal orthologous candidate genes and or pathways that contribute not only to SCLS, but also to normal and dysregulated mechanisms underling vascular barrier function more generally.

MATERIALS AND METHODS

Animals. AKR/J (AKR), BPL/1J, C3H/HeJ (C3H), C3H/HeN, CAST/EiJ, C57BL/6J (B6), CBA/J (CBA), CBA/N, CZECHII/EiJ, I/LnJ, JF1/MsJ, MOLD/EiJ, MOLF/EiJ (MOLF), MRL/MpJ (MRL), MSM/Ms, PWD/PhJ, PWK/PhJ (PWK), RF/J, SF/CamEiJ, and SKIVE/EiJ were purchased from the Jackson Laboratory (Bar Harbor, Maine). B6.129P-*Hrh1*^{tm1Wat} (HRH1KO) [31], C3H.*Bphs*^{SJL} (C3H.*Bphs*^{S}) [15], (B6 × HRH1KO) F_1, (C3H × HRH1KO) F_1, (CBA × HRH1KO) F_1, (AKR × HRH1KO) F_1, (MRL × HRH1KO) F_1, (AKR × PWK) F_1, (C3H × MOLF) F_1, (MOLF × HRH1KO) × HRH1KO, (AKR × PWK) × AKR, (C3H × MOLF) × C3H, C3H.*Bphs*$^{MOLF+/-}$, C3H.*Bphse*^{C3H}, AKR.*Bphse*$^{PWK+/-}$ and AKR.*Bphse*^{AKR} were generated and maintained under specific pathogen free conditions in the vivarium of the Given Medical Building at the University of Vermont according to National Institutes of Health guidelines. All animal studies were approved by the Institutional Animal Care and Use Committee of the University of Vermont.

Bphs Phenotyping. Bphs phenotyping was carried out as previously described [15]. Briefly, mice were injected with purified PTX (List Biological Laboratories, Inc.) in 0.025 M Tris buffer containing 0.5 M NaCl and 0.017% Triton X-100, pH 7.6. Control animals received carrier. Three days later, mice were challenged by injection with histamine (milligrams per kilogram of body weight [dry weight], free base) suspended in phosphate-buffered saline (PBS). Deaths were recorded at 30 min post-challenge. The results are expressed as the number of animals dead over the number of animals studied.

DNA sequencing of third intracellular loop of *Hrh1*. DNA for 91 inbred laboratory and wild-derived strains of mice was purchased from the Mouse DNA resource at The Jackson Laboratory (www.jax.org) and used in an *Hrh1* specific PCR reaction

using the following primer sets: forward-740F, 5'-TGCCAAGAAACCTGGGAAAG-3', and reverse-1250R, 5'-CAACTGCTTGGCTGCCTTC-3' that amplify the third intracellular loop of *Hrh1*. Thermocycling was carried out for a 15 µl reaction mix with 2 mM MgCl2, 200 µM dNTPs, 0.2 µM primers, 1 unit of Taq polymerase and ~50 ng of genomic DNA together with an initial 2-min 97°C denaturation followed by 35 cycles of 97°C for 30 sec, 58°C for 30 sec and 72°C for 30 sec. The final extension was for 5 min at 72°C. *Hrh1* amplicons from each mouse strain were gel purified (Qiagen Cat# 28115) and DNA sequencing reactions were performed with the BigDye terminator cycle sequencing kit (Applied Biosystems, Foster City, CA) using 740F or 1250F reverse primers. The reaction products were resolved on an ABI Prism 3100 DNA sequencer at the DNA analysis facility at the University of Vermont. DNA sequencing data were assembled and analyzed using MultiAlign [58]. Each potential nucleotide sequence polymorphism was confirmed by comparing it with the actual chromatographic profiles using Chromas v2.6.5 (https://technelysium.com.au/wp/)

DNA isolation and genotyping. DNA was isolated from mouse tail clippings as previously described [13]. Briefly, individual tail clippings were incubated with cell lysis buffer (125 mg/ml proteinase K, 100 mM NaCl, 10 mM Tris-HCl (pH 8.3), 10 mM EDTA, 100 mM KCl, 0.50% SDS, 300 ml) overnight at 55ºC. The next day, 6M NaCl (150 ml) was added followed by centrifugation for 10 min at 4ºC. The supernatant layer was transferred to a fresh tube containing 300 µl isopropanol. After centrifuging for 2 min, the supernatant was discarded, and the pellet washed with 70% ethanol. After a final 2 min centrifugation, the supernatant was discarded, and DNA was air dried and resuspended

in TE. Genotyping was performed using microsatellite, sequence specific, and *Hrh1* primers (**Supplemental Table 5**).

Microsatellite primers: Polymorphic microsatellites were selected to have a minimum polymorphism of 8 bp for optimal identification by agarose gel electrophoresis. Briefly, primers were synthesized by IDT-DNA (Coralville, IA) and diluted to a concentration of 10 uM. PCR amplification was performed using Promega GoTaq according standard conditions and amplicons were subjected to 2% agarose gel electrophoresis and visualized by ethidium bromide and UV light.

Sequence-specific primers: Genotyping was performed using sequence specific primers that differ only at the 3' nucleotide corresponding to each allele of the identified SNP [59]. Each primer set was designed using Primer3 to have a Tmelt of 58-60°C and synthesized by IDT-DNA (Coralville, IA) and used at a concentration of 100 uM. PCR reactions were subjected to cycling conditions as described and if found to be necessary, the annealing temperature at each stage was adjusted to accommodate the optimal Tmelt. Amplicons were electrophoresed with 10 ul Orange G loading buffer on a 1.5% agarose gel stained with ethidium bromide and visualized by UV light. The presence of a SNP specific allele was scored by observing an amplicon of the expected size in either reaction.

HRH1KO mice genotyping: Wild-type and *Hrh1*$^{-/-}$ alleles were genotyped as previously described [15]. Approximately 60 ng of DNA was amplified (GeneAmp PCR system 9700, Applied Biosystems, Foster City, CA). The DNA was amplified by incubation at 94°C for 3 min followed by 35 cycles of 94°C for 30 sec, 62°C for 30 sec, and 72°C for 30 sec. At the end of the 35 cycles, the DNA was incubated at 72°C for 10 min and 4°C

for 10 min. The amplified DNA was analyzed by gel electrophoresis in a 1.5% agarose gel. The DNA was visualized by staining with ethidium bromide.

Linkage analysis and generation of *Bphse* congenic. Segregation of genotype frequency differences with susceptibility and resistance to Bphs in (MOLF × HRH1KO) × HRH1KO and (AKR × PWK) × AKR mice were tested by χ^2 in 2 × 2 contingency tables. C3H.*Bphse*$^{MOLF+/-}$, C3H.*Bphse*^{C3H}, AKR.*Bphse*$^{PWK+/-}$ and AKR.*Bphse*^{AKR} congenic mice were derived by marker assisted selection. (AKR × PWK) × AKR and (C3H × MOLF) × C3H mice that were heterozygous across the *Bphse* interval at N2 and at each successive BC generation were selected for continued breeding. *Bphse* congenic mice were maintained as heterozygotes.

Low-resolution interval-specific targeted genetic association testing. Genotype data (SNPs in both coding and non-coding) of 50 mouse strains (**Supplementary Table 1**) that were phenotyped for Bphs either by us or described in the literature [12, 15, 17, 19, 40], was retrieved from public databases at the Sanger Institute (https://www.sanger.ac.uk/science/data/mouse-genomes-project) and The Jackson Laboratory (https://phenome.jax.org/). The lack of representation of several inbred strains especially wild-derived strains in these databases were compensated by genotyping using chromosome region capture sequencing [59] as follows:

*DNA Fragmentation***:** For chromosome region capture sequencing, 3 *μ*g of genomic DNA from BPN/3J, BPL/1J, CASA/RkJ, CAST/EiJ, CBA/J, C3H/HeN, CZECHII/EiJ, JF1/Ms, MOLD/EiJ, MOLF/EiJ, MRL/MpJ, MSM/Ms, NU/J, PWD/PhJ, SF/CamEiJ and SKIVE/EiJ mice was sheared into fragments of approximately 200 bp with the Covaris E220 system (Covaris, USA). The sheared DNA fragments were then

purified for each of the 16 mice strains using AMPure XP Beads (Beckman, USA), following the instructions of the reagent supplier.

DNA Library Construction: DNA libraries of the purified fragments were constructed with SureSelect Library Prep Kit (Agilent, USA). In brief, DNA end-repair was performed for the fragments from each muse strain using 10× End Repair Buffer, dNTP Mix, T4 DNA Polymerase, Klenow DNA Polymerase, and T4 Polynucleotide Kinase. After incubation of the mixture at 20 °C for 30 min, Addition of nucleotide A at the 3' end of the sequence was performed using 10×Klenow Polymerase Buffer, dATP and Exo(-) Klenow, at 37 °C for 30 min. Ligation reaction was then conducted using T4 DNA Ligase Buffer, SureSelect Adaptor Oligo Mix, and T4 DNA Ligase at 20 °C for 15 min. The adaptor-ligated library was finally amplified through using SureSelect Primer, SureSelect ILM Indexing Pre Capture PCR Reverse Primer, 5X Herculase II Rxn Buffer, 100 mM dNTP Mix, and Herculase II Fusion DNA Polymerase. The condition for the amplification was fixed as: initial denaturation at 98°C for 2 min, followed by 30 cycles of reactions at 98 °C for 30 Sec, 65 °C annealing for 30 Sec, 72 °C extension 30 Sec. Purification of the amplified products was performed with 1.8X Agencourt AMPure XP beads for each of the libraries. The average insert length for the adaptor-ligated libraries ranged between 225 ~ 275bps.

Hybridization capture: The libraries were subjected for the hybridization capture using the SureSelect Target Enrichment Kit (Agilent, USA), following the instruction of the reagent supplier. The prepared library were then reacted with SureSelect Block Mix at 95 °C for 5min, followed by holding at 65 °C, and the Hybridization Buffer plus capture library mix were added and maintained at 65 °C for 24hrs. Finally, Dynabeads

M-280 streptavidin (Life, USA) was used for the enrichment of the Captured DNA libraries **[**60**,** 61**].**

Index amplification: For each enriched captured DNA library, the index amplification was performed with 5X Herculase II Rxn Buffer, 100 mM dNTP Mix, SureSelect ILM Indexing Post Capture Forward PCR Primer, and Herculase II Fusion DNA Polymerase. The reaction procedure was: 98°C Pre-denaturation for 2 Min, 98 °C denaturation for 30 Sec, 57 °C annealing for 30 Sec, 72 °C extension for 30 Sec, amplification for 12 rounds, followed by purification using 1.8 times the volume of AMPure XP Beads. DNA libraries of 250-350 bp range were obtained for the subsequent sequencing [60].

DNA Sequencing: A 10 ng library was used for cluster generation in cBot with the TruSeq PE Cluster Kit (illumina, USA) followed by bidirectional sequencing in an Illumina Hiseq 2500 to obtain the data of 2x150 bp.

Data processing and SNP calls: To ensure the quality of subsequent information analysis, the original sequence was filtered with the software SolexaQA to get high quality Clean Reads [62]. Efficient high-quality sequencing data was mapped to the reference genome mm10 by the BWA software [63], samtools [64] was used for sorting, picard tools was used for duplicate read removal, and GATK was used for realignment around indels and base quality score recalibration [65]. Finally, GATK HaplotypeCaller was used for SNP detection.

All SNP datasets (MPD, Chromosome region capture sequencing) were collated to yield a total of 1,303,072 SNPs across the Bphse interval (Chr6: 59-129 Mb), among which 13,257 SNPs had 100% coverage (no missing genotypes) across all strains.

To calculate associations between genetic polymorphisms and Bphs, we used efficient mixed-model association (EMMA) [38]. This method treats genetic relatedness as a random variable in a linear mixed model to account for population structure, thereby reducing false associations between SNPs and the measured trait. We used the likelihood ratio test function (emma.ML.LRT) to generate *p*-values. Significance was assessed with Bonferroni multiple correction testing. The -log transformed *p*-values were plotted using GraphPad Prism7 and genomic coordinates included for each SNP using the latest mouse genome build GRCm38.p5/mm10.

Genotype imputation methodology. A merged SNP dataset over the Chr6 region 111.0-116.4 Mb (GRCm38 / mm10 and dbSNP build 142) was constructed from the 11 SNP genotyping datasets available (see **Supplementary Table 6**) on the Mouse Phenome Database (MPD) [41, 42, 66-71]. This MPD-derived merged genotype dataset of 577 strains was then merged with the genotype data for 50 strains generated earlier for low resolution mapping (see "low resolution interval-specific targeted genetic association testing"). We leveraged the genotype data from over 577 strains to impute genotypes for missing SNP states across the region for the 50 strains of interest (see **Supplementary Table 1**). To impute genotypes on a target strain, we utilized the Viterbi algorithm implemented in HaploQA [41, 42] where the input was a subset of strains most phylogenetically similar to the target strain. This imputation strategy resulted in a dataset of 78,334 SNPs in the genomic region of interest. Across all 50 strains, the median number of missing SNP genotypes after imputation was 2.45% with a maximum missing of only 5.4% for one of the strains.

Trait-related gene sets. The positional candidate genes were ranked based on their predicted association with seven functional terms related to the Bphs phenotype: “Cardiac", “G-protein coupled receptor", “Histamine", “Pertussis toxin", “Type I hypersensitivity", “Vascular Permeability", and “ER/EMC/ERAD”. Gene Weaver [72] was used to identify genes annotated with each term. Each term was entered the Gene Weaver homepage (https://geneweaver.org)and search restricted to human, rat, and mouse genes, and to curated lists only. Mouse homologs for each gene were retrieved using the batch query tool in MGI (http://www.informatics.jax.org/batch_data.shtml). In addition, using the Gene Expression Omnibus (GEO) and PubMed, additional gene expression data sets were retrieved for each phenotype term. Final gene lists consisted of the unique set of genes associated with each process term.

Functional enrichment and ranking of Bphs associated genes. We associated genes with Bphs-related functions as described in Tyler *et al.* [34]. Briefly, we used the connectivity weights in the Functional Network of Tissues in Mouse (FNTM) as features for training support vector machines [73]. Each feature consisted of the connection weights from a given gene to genes in the functional module. To improve classification and reduce over-generalization we clustered each functional gene set into modules, each less than 400 genes [43]. For each of these modules, we trained 100 SVMs to classify the module genes from a balanced set of randomly chosen genes from outside the module. We used 10-fold cross validation and a linear kernel. We also trained each SVM over a series of cost parameters identified by iteratively narrowing the cost parameter window to identify a series of eight cost parameters that maximized classification accuracy. We then used the training modules to score each positional candidate gene in the *Bphse* locus.

To compare scores across multiple trained models, we converted SVM scores to false positive rates.

Combined gene score. To create the final ranked list of positional candidate genes, we combined the SNP association scores with the functional predictions derived from the SVMs. We scaled each of these scores by its maximum value across all positional candidates and summed them together to derive a combined gene score (S_{cg}) that incorporated both functional predictions and genetic influence:

where the denominators of the two terms on the right-hand side are the maximum values of $-\log_{10}(pEMMA)$ and $-\log_{10}(FPR_{SVM})$ over all positional candidates in *Bphse*, respectively, which normalizes the functional and positional scores to be comparable to each other. SNPs were assigned to the nearest gene within 1Mb. If more than one SNP was assigned to a gene, we used the maximum negative $\log_{10}$ *p* value among all SNPs assigned to the gene.

ACKNOWLEDGEMENTS

Anna Tyler and Mathew Mahoney are supported by a grant (R21 LM012615) from the National Library of Medicine of the United States National Institutes of Health (NIH). Abbas Raza, Dimitry Krementsov, Elizabeth Blankenhorn, and Cory Teuscher were supported by grants from the NIH and the National Multiple Sclerosis Society (NMSS). Dimitry Krementsov was supported by NIH grants from the National Institute of Neurological Disease and Stroke (R01 NS097596), National Institute of Allergy and Infectious Disease (R21 AI145306), and the NMSS (RR-1602-07780).

We would like to thank Keith Sheppard and Molly Bogue for their assistance with genomic imputation as well as the Mouse Phenome Database web resource (RRID:SCR_003212). We also are grateful for the assistance of Laura Cort in the genotyping of the backcross progeny.

REFERENCES

1. Panula, P., et al., *International Union of Basic and Clinical Pharmacology. XCVIII. Histamine Receptors.* Pharmacol Rev, 2015. **67**(3): p. 601-55.
2. Parsons, M.E. and C.R. Ganellin, *Histamine and its receptors.* Br J Pharmacol, 2006. **147 Suppl 1**: p. S127-35.
3. Branco, A., et al., *Role of Histamine in Modulating the Immune Response and Inflammation.* Mediators Inflamm, 2018. **2018**: p. 9524075.
4. Moya-Garcia, A.A., et al., *Histamine, Metabolic Remodelling and Angiogenesis: A Systems Level Approach.* Biomolecules, 2021. **11**(3).
5. Peavy, R.D. and D.D. Metcalfe, *Understanding the mechanisms of anaphylaxis.* Curr Opin Allergy Clin Immunol, 2008. **8**(4): p. 310-5.
6. Emanuel, M.B., *Histamine and the antiallergic antihistamines: a history of their discoveries.* Clin Exp Allergy, 1999. **29 Suppl 3**: p. 1-11; discussion 12.
7. Lee, M.R., *The history of ergot of rye (Claviceps purpurea) II: 1900-1940.* J R Coll Physicians Edinb, 2009. **39**(4): p. 365-9.
8. Lee, M.R., *The history of ergot of rye (Claviceps purpurea) I: from antiquity to 1900.* J R Coll Physicians Edinb, 2009. **39**(2): p. 179-84.
9. Windaus, A. and W. Vogt, *Synthese des Imidazolyl-äthylamins.* Berichte der deutschen chemischen Gesellschaft, 1907. **40**(3): p. 3691-3695.
10. Barger, G. and H.H. Dale, *The presence in ergot and physiological activity of beta-imidazolylethylamine*. 1910.
11. Dale, H.H. and P.P. Laidlaw, *The physiological action of β-iminazolylethylamine.* The Journal of physiology, 1910. **41**(5): p. 318-344.
12. Munoz, J. and R.K. Bergman, *Histamine-sensitizing factors from microbial agents, with special reference to Bordetella pertussis.* Bacteriol Rev, 1968. **32**(2): p. 103-26.
13. Parfentjev, I.A. and M.A. Goodline, *Histamine shock in mice sensitized with Hemophilus pertussis vaccine.* J Pharmacol Exp Ther, 1948. **92**(4): p. 411-3.
14. Sudweeks, J.D., et al., *Locus controlling Bordetella pertussis-induced histamine sensitization (Bphs), an autoimmune disease-susceptibility gene, maps distal to T-*

cell receptor beta-chain gene on mouse chromosome 6. Proc Natl Acad Sci U S A, 1993. **90**(8): p. 3700-4.

15. Ma, R.Z., et al., *Identification of Bphs, an autoimmune disease locus, as histamine receptor H1.* Science, 2002. **297**(5581): p. 620-3.
16. Iff, E.T. and N.M. Vaz, *Mechanisms of anaphylaxis in the mouse. Similarity of shock induced by anaphylaxis and by mixtures of histamine and serotonin.* Int Arch Allergy Appl Immunol, 1966. **30**(4): p. 313-22.
17. Diehl, S.A., et al., *G proteins Galphai1/3 are critical targets for Bordetella pertussis toxin-induced vasoactive amine sensitization.* Infect Immun, 2014. **82**(2): p. 773-82.
18. Katada, T. and M. Ui, *ADP ribosylation of the specific membrane protein of C6 cells by islet-activating protein associated with modification of adenylate cyclase activity.* J Biol Chem, 1982. **257**(12): p. 7210-6.
19. Gao, J.F., et al., *Analysis of the role of Bphs/Hrh1 in the genetic control of responsiveness to pertussis toxin.* Infect Immun, 2003. **71**(3): p. 1281-7.
20. Wardlaw, A.C., *Inheritance of responsiveness to pertussis HSF in mice.* Int Arch Allergy Appl Immunol, 1970. **38**(6): p. 573-89.
21. Noubade, R., et al., *Autoimmune disease-associated histamine receptor H1 alleles exhibit differential protein trafficking and cell surface expression.* J Immunol, 2008. **180**(11): p. 7471-9.
22. Petkov, P.M., et al., *An efficient SNP system for mouse genome scanning and elucidating strain relationships.* Genome Res, 2004. **14**(9): p. 1806-11.
23. Poltorak, A., S. Apalko, and S. Sherbak, *Wild-derived mice: from genetic diversity to variation in immune responses.* Mamm Genome, 2018. **29**(7-8): p. 577-584.
24. Bearoff, F., et al., *Natural genetic variation profoundly regulates gene expression in immune cells and dictates susceptibility to CNS autoimmunity.* Genes Immun, 2016. **17**(7): p. 386-395.
25. Dejager, L., C. Libert, and X. Montagutelli, *Thirty years of Mus spretus: a promising future.* Trends Genet, 2009. **25**(5): p. 234-41.
26. Harper, J.M., *Wild-derived mouse stocks: an underappreciated tool for aging research.* Age (Dordr), 2008. **30**(2-3): p. 135-45.

27. Guenet, J.L. and F. Bonhomme, *Wild mice: an ever-increasing contribution to a popular mammalian model.* Trends Genet, 2003. **19**(1): p. 24-31.
28. Bult, C.J., et al., *Mouse Genome Database (MGD) 2019.* Nucleic Acids Res, 2019. **47**(D1): p. D801-d806.
29. Beck, J.A., et al., *Genealogies of mouse inbred strains.* Nat Genet, 2000. **24**(1): p. 23-5.
30. Boursot, P., et al., *The Evolution of House Mice.* Annual Review of Ecology and Systematics, 1993. **24**(1): p. 119-152.
31. Inoue, I., et al., *Impaired locomotor activity and exploratory behavior in mice lacking histamine H1 receptors.* Proc Natl Acad Sci U S A, 1996. **93**(23): p. 13316-20.
32. Graber, J.H., et al., *Patterns and mechanisms of genome organization in the mouse.* J Exp Zool A Comp Exp Biol, 2006. **305**(9): p. 683-8.
33. Petkov, P.M., et al., *Evidence of a large-scale functional organization of mammalian chromosomes.* PLoS Genet, 2005. **1**(3): p. e33.
34. Tyler, A.L., et al., *Network-Based Functional Prediction Augments Genetic Association To Predict Candidate Genes for Histamine Hypersensitivity in Mice.* G3 (Bethesda), 2019. **9**(12): p. 4223-4233.
35. Raza, A., et al., *A natural mouse model reveals genetic determinants of systemic capillary leak syndrome (Clarkson disease).* Commun Biol, 2019. **2**: p. 398.
36. Grubb, S.C., et al., *Mouse phenome database.* Nucleic Acids Res, 2009. **37**(Database issue): p. D720-30.
37. Adams, D.J., et al., *The Mouse Genomes Project: a repository of inbred laboratory mouse strain genomes.* Mamm Genome, 2015. **26**(9-10): p. 403-12.
38. Kang, H.M., et al., *Efficient control of population structure in model organism association mapping.* Genetics, 2008. **178**(3): p. 1709-23.
39. Munoz, J. and L.F. Schuchardt, *Studies on the sensitivity of mice to histamine following injection of hemophilus pertussis. I. Effect of strain and age of mice.* J Allergy, 1953. **24**(4): p. 330-4.

40. Linthicum, D.S. and J.A. Frelinger, *Acute autoimmune encephalomyelitis in mice. II. Susceptibility is controlled by the combination of H-2 and histamine sensitization genes.* J Exp Med, 1982. **156**(1): p. 31-40.
41. Morgan, A.P., et al., *The Mouse Universal Genotyping Array: From Substrains to Subspecies.* G3 (Bethesda), 2015. **6**(2): p. 263-79.
42. 1/1/2020]; Available from: https://github.com/TheJacksonLaboratory/haploqa.
43. Guan, Y., et al., *Functional genomics complements quantitative genetics in identifying disease-gene associations.* PLoS Comput Biol, 2010. **6**(11): p. e1000991.
44. Munoz, J. and R.K. Bergman, *Mechanism of Anaphylactic Death in the Mouse.* Nature, 1965. **205**: p. 199-200.
45. Wang, M., et al., *Mouse anaphylactic shock is caused by reduced cardiac output, but not by systemic vasodilatation or pulmonary vasoconstriction, via PAF and histamine.* Life Sci, 2014. **116**(2): p. 98-105.
46. Seifert, R., et al., *Molecular and cellular analysis of human histamine receptor subtypes.* Trends Pharmacol Sci, 2013. **34**(1): p. 33-58.
47. Fink, M.A. and M.V. Rothlauf, *Variations in sensitivity to anaphylaxis and to histamine in inbred strains of mice.* Proc Soc Exp Biol Med, 1954. **85**(2): p. 336-8.
48. Lu, C., et al., *Endothelial histamine H1 receptor signaling reduces blood-brain barrier permeability and susceptibility to autoimmune encephalomyelitis.* Proc Natl Acad Sci U S A, 2010. **107**(44): p. 18967-72.
49. Meeker, N.D., et al., *Physical mapping of the autoimmune disease susceptibility locus, Bphs: co-localization with a cluster of genes from the TNF receptor superfamily on mouse chromosome 6.* Mamm Genome, 1999. **10**(9): p. 858-63.
50. Kelly, N.J., et al., *Mouse Genome-Wide Association Study of Preclinical Group II Pulmonary Hypertension Identifies Epidermal Growth Factor Receptor.* Am J Respir Cell Mol Biol, 2017. **56**(4): p. 488-496.
51. Klein, A.D., et al., *Identification of Modifier Genes in a Mouse Model of Gaucher Disease.* Cell Rep, 2016. **16**(10): p. 2546-2553.
52. Chitwood, P.J., et al., *EMC Is Required to Initiate Accurate Membrane Protein Topogenesis.* Cell, 2018. **175**(6): p. 1507-1519 e16.

53. Hoyer, M.J., et al., *A Novel Class of ER Membrane Proteins Regulates ER-Associated Endosome Fission.* Cell, 2018. **175**(1): p. 254-265 e14.
54. Noh, S.H., et al., *Specific autophagy and ESCRT components participate in the unconventional secretion of CFTR.* Autophagy, 2018. **14**(10): p. 1761-1778.
55. Tachibana, M., et al., *Activation of peroxisome proliferator-activated receptor gamma suppresses mast cell maturation involved in allergic diseases.* Allergy, 2008. **63**(9): p. 1136-47.
56. Ushio, H., et al., *Crucial role for autophagy in degranulation of mast cells.* J Allergy Clin Immunol, 2011. **127**(5): p. 1267-76 e6.
57. Son, N.H., et al., *Cardiomyocyte expression of PPARgamma leads to cardiac dysfunction in mice.* J Clin Invest, 2007. **117**(10): p. 2791-801.
58. Corpet, F., *Multiple sequence alignment with hierarchical clustering.* Nucleic Acids Res, 1988. **16**(22): p. 10881-90.
59. Bunce, M., et al., *Phototyping: comprehensive DNA typing for HLA-A, B, C, DRB1, DRB3, DRB4, DRB5 & DQB1 by PCR with 144 primer mixes utilizing sequence-specific primers (PCR-SSP).* Tissue Antigens, 1995. **46**(5): p. 355-67.
60. Gnirke, A., et al., *Solution hybrid selection with ultra-long oligonucleotides for massively parallel targeted sequencing.* Nat Biotechnol, 2009. **27**(2): p. 182-9.
61. Mamanova, L., et al., *Target-enrichment strategies for next-generation sequencing.* Nat Methods, 2010. **7**(2): p. 111-8.
62. Cox, M.P., D.A. Peterson, and P.J. Biggs, *SolexaQA: At-a-glance quality assessment of Illumina second-generation sequencing data.* BMC Bioinformatics, 2010. **11**: p. 485.
63. Li, H. and R. Durbin, *Fast and accurate short read alignment with Burrows-Wheeler transform.* Bioinformatics, 2009. **25**(14): p. 1754-1760.
64. Li, H., et al., *The Sequence Alignment/Map format and SAMtools.* Bioinformatics, 2009. **25**(16): p. 2078-9.
65. McKenna, A., et al., *The Genome Analysis Toolkit: a MapReduce framework for analyzing next-generation DNA sequencing data.* Genome Res, 2010. **20**(9): p. 1297-303.

66. Kirby, A., et al., *Fine mapping in 94 inbred mouse strains using a high-density haplotype resource.* Genetics, 2010. **185**(3): p. 1081-95.
67. Yang, H., et al., *Subspecific origin and haplotype diversity in the laboratory mouse.* Nat Genet, 2011. **43**(7): p. 648-55.
68. Frazer, K.A., et al., *A sequence-based variation map of 8.27 million SNPs in inbred mouse strains.* Nature, 2007. **448**(7157): p. 1050-3.
69. Keane, T.M., et al., *Mouse genomic variation and its effect on phenotypes and gene regulation.* Nature, 2011. **477**(7364): p. 289-94.
70. Eskin, E. 6/25/2020]; Available from: http://mouse.cs.ucla.edu/mousehapmap/beta/index.html.
71. Srivastava, A., et al., *Genomes of the Mouse Collaborative Cross.* Genetics, 2017. **206**(2): p. 537-556.
72. Baker, E.J., et al., *GeneWeaver: a web-based system for integrative functional genomics.* Nucleic Acids Res, 2012. **40**(Database issue): p. D1067-76.
73. Goya, J., et al., *FNTM: a server for predicting functional networks of tissues in mouse.* Nucleic Acids Res, 2015. **43**(W1): p. W182-7.

Table 1. Distribution of *Hrh1*^{s} and *Hrh1*^{r} alleles in laboratory and wild-derived inbred mouse strains.

Susceptible Haplotype (Pro^{263}, Val^{312}, Pro^{330}) *Hrh1*^{s}			**Resistant Haplotype (Leu^{263}, Met^{312}, Ser^{330}) *Hrh1*^{r}**
129X1/SvJ	C57BR/cdJ	P/J	AKR/J
129S1/SvImJ	C57L/J	PANCEVO/EiJ	BPL/1J
129T2/SvEmsJ	C58/J	PERA/EiJ	C3H/HeJ
A/HeJ	CALB/RkJ	PERC/EiJ	C3H/HeN
A/J	CE/E	PL/J	CASA/RkJ
A/WySnJ	DBA/1J	RBF/DnJ	CAST/EiJ
ALR/LtJ	DBA/2J	RIIIS/J	CBA/J
ALS/LtJ	DDY/JclSidSeyFrkJ	SB/LeJ	CBA/N
B10.S/DvTee	EL/SuzSeFrkJ	SEA/GnJ	CZECHI/EiJ
B10.S/McdgJ	FVB/NCr	SEC/1ReJ	CZECHII/EiJ
BALB/cByJ	IS/CamRkJ	SENCARA/PtJ	I/LnJ
BALB/cJ	KK/HIJ	SENCARB/PtJ	JF1/Ms
BDP/J	LEWES/EiJ	SENCARC/PtJ	MOLC/RkJ
BPH/2J	LG/J	SJL/J	MOLD/RkJ
BPL/1J	LP/J	SJL/BmJ	MOLF/EiJ
BPN/3J	MA/MyJ	SM/J	MRL/MpJ
BTBRT+	MOR/RkJ	SPRET/EiJ	MSM/Ms
BXSB/MpJ	NOD/LtJ	ST/BJ	PWD/PhJ
C57BL/10J	NON/LtJ	SWR/J	PWK/PhJ
C57BL/10SnJ	NOR/LtJ	SWXL-4/TyJ	RF/J
C57BL/6ByJ	NZB//BINJ	TIRANO/EiJ	SF/CamEiJ
C57BL/6J	NZO/HILtJ	YBR/EiJ	SKIVE/EiJ
C57BLKS/J	NZW/LacJ	ZALENDE/EiJ	

Table 2. Bphs susceptibility of mice with the *Hrh1*^{r}/HRH1^{r} allele.

		Histamine (mg/kg)					
Strain	**Group**[a]	**100**	**50**	**25**	**Total**	**% Aff**	***p*-value**[b]
C3H/HeJ	1	0/3	0/2	0/2	0/7	0	
C3H/HeN	1	0/2	0/2	0/2	0/6	0	
C3H		0/5	0/4	0/4	0/13	0	
AKR/J	1	1/3	0/2	0/2	1/7	14	0.4
CAST/EiJ	7	1/3	0/3	0/3	1/9	11	0.4
CBA/J	1	0/3	0/2	0/2	0/7	0	
CBA/N	1	0/3	0/2	0/2	0/7	0	
CBA		0/6	0/4	0/4	0/14	0	1.0
I/LnJ	6	2/7	0/3	-	2/10	20	0.2
MSM/Ms	7	0/3	0/3	-	0/6	0	1.0
MRL/MpJ	1	0/3	0/2	0/2	0/7	0	1.0
SF/CamEiJ	1	0/4	0/2	-	0/6	0	1.0
SKIVE/EiJ	7	2/7	1/6	0/2	3/15	20	0.2
BPL/1J	5	1/2	2/2	2/2	5/6	83	0.0005
CZECHII/EiJ	7	4/4	2/4	2/2	8/10	80	<0.0001
JF1/MsJ	7	2/3	2/3	-	4/6	67	0.004
MOLD/EiJ	7	2/2	1/2	2/2	5/6	83	0.0005
MOLF/EiJ	7	2/2	5/5	5/5	12/12	100	<0.0001
PWD/PhJ	7	5/7	-	-	5/7	71	0.001
PWK/PhJ	7	2/2	2/2	2/2	6/6	100	<0.0001
RF/J	1	2/2	2/2	2/2	6/6	86	<0.0001

Mice were injected with 200 ng of PTX on D0. Three days later the animals were challenged with the indicated dose of HA (mg dry weight free base/kg body weight) by intraperitoneal injection and deaths recorded as number of animals dead/number of animals tested at 30 minutes post HA challenge. [a] according to mouse family tree (adapted from Petkov *et al*. [22]). [b] Relative to C3H mice

Table 3. Bphs susceptibility of *Hrh1*^{s} and *Hrh1*^{r} by HRH1KO F_1 hybrid mice.

	Histamine (mg/kg)							
Strain	**100**	**50**	**25**	**12.5**	**6.25**	**Total**	**% Aff**	***p*-value[a]**
HRH1KO	0/2	0/2	0/2	0/2	0/2	0/10	0	
C57BL/6J	3/3	3/3	3/3	2/2	1/2	12/15	90	<0.0001
(B6 × HRH1KO) F_1	4/4	4/4	4/4	3/4	3/3	18/19	95	<0.0001
C3H.*Bphs*^{SJL}	3/3	2/2	2/2	2/2	2/2	11/11	100	<0.0001
(*Bphs*^{SJL} × HRH1KO) F_1	2/2	2/2	2/2	2/2	2/2	10/10	100	<0.0001
C3H/HeJ	1/3	0/2	0/2	0/2	0/2	1/11	9	
(C3H × HRH1KO) F_1	0/2	0/2	0/2	0/2	0/2	0/10	0	
CBA/J	0/3	0/2	0/2	0/2	0/2	0/11	0	
(CBA x HRH1KO) F_1	0/2	0/3	0/2	0/2	0/2	0/11	0	
AKR/J	1/3	0/2	0/2	0/2	0/2	1/11	9	
(AKR x HRH1KO) F_1	0/2	0/2	0/2	0/2	0/2	0/10	0	
MRL/MpJ	0/3	0/2	0/2	0/2	0/2	0/11	0	
(MRL x HRH1KO) F_1	2/3	0/2	0/2	0/2	0/2	2/11	18	
PWK/PhJ	3/3	3/3	2/2	1/2	0/2	9/12	75	0.0005
(PWK x HRH1KO) F_1	3/3	2/2	2/2	1/2	1/2	11/13	85	<0.0001
MOLF/MpJ	2/2	2/2	2/2	2/2	0/2	8/10	80	<0.0001
(MOLF x HRH1KO) F_1	2/2	2/2	2/2	2/2	0/2	8/10	80	<0.0001
(MOLF x HRH1KO) x HRH1KO	114	**Aff**	**Unaff**					
HRH1$^{-/-}$	54	0	54			0/54	0%	
HRH1$^{MOLF/-}$	60	54	6			54/60	90%	<0.0001

Mice were injected with 200 ng of PTX on D0. Three days later the animals were challenged with the indicated dose of HA (mg dry weight free base/kg body weight) by intraperitoneal injection and deaths recorded as number of animals dead/number of animals tested at 30 minutes post HA challenge. [a]Relative to HRH1KO mice

Table 4. Linkage of Chr6 marker loci to *Bphse*.

Marker	bp	χ2	*p*-value	A Ho	A He	Un Ho	Un He	Total
rs36385580	59,353,905	28.8	7.95E-08	28	52	65	20	165
rs38650989	72,592,521	30.6	3.21E-08	28	52	66	19	165
D6Mit186	73,387,511	29.5	5.49E-08	30	53	66	19	168
D6Mit102	93,463,949	38.2	6.36E-10	25	58	66	19	168
D6Mit65	101,387,523	42.3	7.92E-11	25	58	68	17	168
D6Mit149	106,005,405	38.5	5.44E-10	27	56	68	17	168
Hrh1	114,397,936							
rs31698248	120,207,163	41.6	1.09E-10	26	56	69	16	167
D6Mit254	125,356,646	35.6	2.42E-09	26	56	66	19	167
rs30853093	125,365,703	34.5	4.32E-09	26	57	65	20	168
rs30662734	125,370,997	34.5	4.32E-09	26	57	65	20	168
rs36868180	127,629,804	32.7	1.06E-08	27	56	65	20	168
D6Mit135	128,834,894	29.2	6.53E-08	27	56	63	22	168

Mice were injected with 200 ng of PTX on D0. Three days later the animals were challenged with the indicated dose of HA (mg dry weight free base/kg body weight) by intraperitoneal injection and deaths recorded as number of animals dead/number of animals tested at 30 minutes post HA challenge. Segregation of genotype frequency differences with $Bphs^s$ (affected = A) and $Bphs^r$ (unaffected = Un) in (AKR × PWK) × AKR mice were tested by χ^2 in 2 × 2 contingency tables. He = AKR/PWK allele, Ho = AKR allele.

Figure 1. Congenic mapping confirms linkage of *Bphse* to *Bphs*/*Hrh1*.

	Marker (bp)													
Strain	***D6Mit74***	***rs36385580 (59,353,905)***	***D6Mit102 (93,463,949)***	***D6Mit65 (101,387,523)***	***D6Mit149 (106,005,405)***	***Hrh1 (114,397,936)***	***D6Mit254 (125,356,646)***	***rs30662734 (125,370,997)***	***rs36868180 (127,629,804)***	***D6Mit135 (128,834,894)***	***D6Mit372 (148,450,482)***	**Bphs**	**% Aff**	***p*-value**
C3H/HeJ	C	C	C	C	C	C	C	C	C	C	C	4/30	13	
MOLF/MpJ	M	M	M	M	M	M	M	M	M	M	M	20/22	90	<0.0001 [a]
C3H.*Bphse*$^{C3H/C3H}$	C	C	C	C	C	C	C	C	C	C	C	7/50	14	
C3H.*Bphse*$^{C3H/MOLF}$	C	He	He	He	He	He	He	He	He	He	C	19/32	60	<0.0002 [a]
AKR/J	A	A	A	A	A	A	A	A	A	A	A	5/30	16	
PWK/J	P	P	P	P	P	P	P	P	P	P	P	15/18	83	<0.0001 [b]
AKR.*Bphse*$^{AKR/AKR}$	A	A	A	A	A	A	A	A	A	A	A	8/47	17	
AKR.*Bphse*$^{AKR/PWK}$	A	He	He	He	He	He	He	He	He	He	A	35/40	88	<0.0001 [b]
C3H+AKR												9/60	15	
MOLF+PWK												35/40	88	<0.0001 [c]
Bphse$^{C3H/C3H}$ +*Bphse*$^{AKR/AKR}$												15/97	15	
Bphse$^{C3H/MOLF}$+*Bphse*$^{AKR/PWK}$												54/72	75	<0.0001 [c]

Mice were injected with 200 ng of PTX on D0. Three days later the animals were challenged with the indicated dose of HA (mg dry weight free base/kg body weight) by intraperitoneal injection and deaths recorded as number of animals dead/number of animals tested at 30 minutes post HA challenge. Marker loci and their location (mm10) are listed along with the respective genotypes: C = C3H, M = MOLF, A = AKR, P = PWK and He = heterozygous. [a]Relative to C3H/HeJ; [b]Relative to AKR/J; [c]Relative to C3H/HeJ and AKR/J combined.

Figure 2. Genetic association with Bphs^{s} was tested using a (**A**) low-resolution 13,257 SNP panel across Chr6:45.0-130.0Mb followed by (**B**) a high-resolution 78,334 imputed SNP panel across Chr6:111.0-116.4 Mb. Both plots show negative log-transformed *p*-values of each SNP tested using Efficient Mixed Model Association (EMMA) on the y-axis. Each filled circle denotes a single SNP. Significance thresholds are shown with a dotted line in each panel. The x-axis denotes Mb coordinates for Chr6 (mm10). (**C**) Gene names are included for SNPs that crossed *p*-value cut-off of 5.00×10^{-3}.

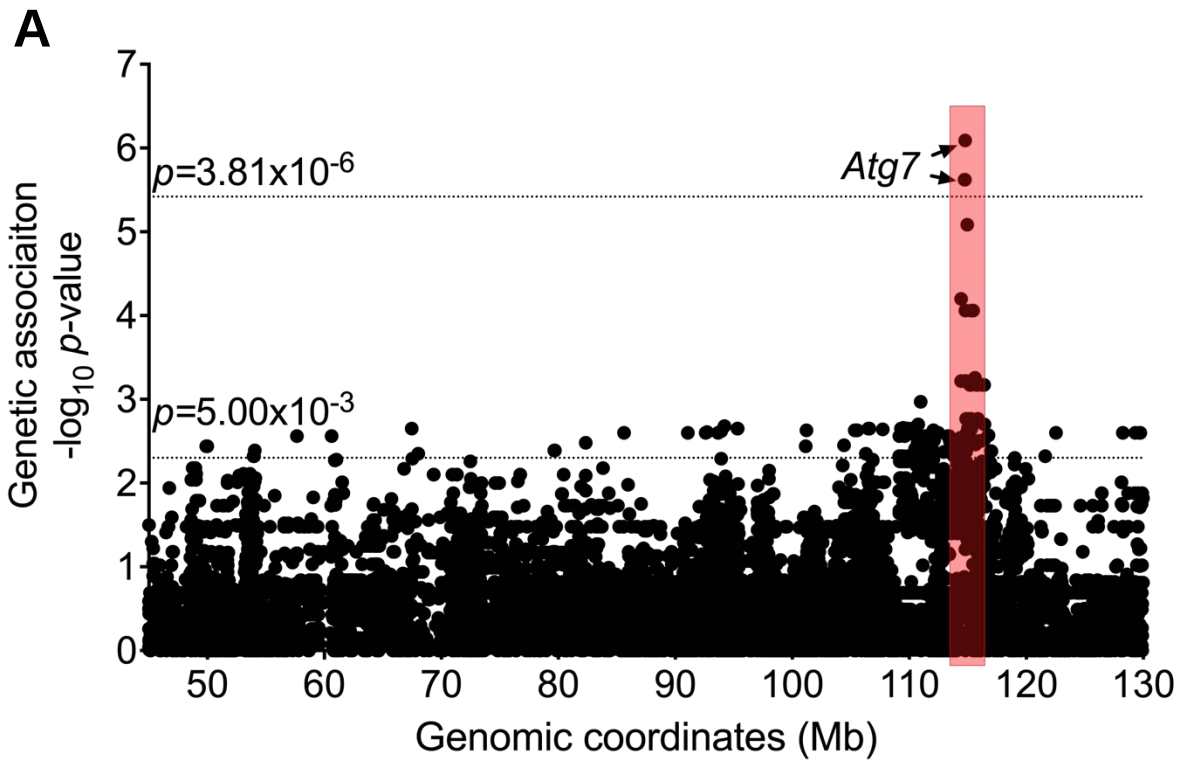

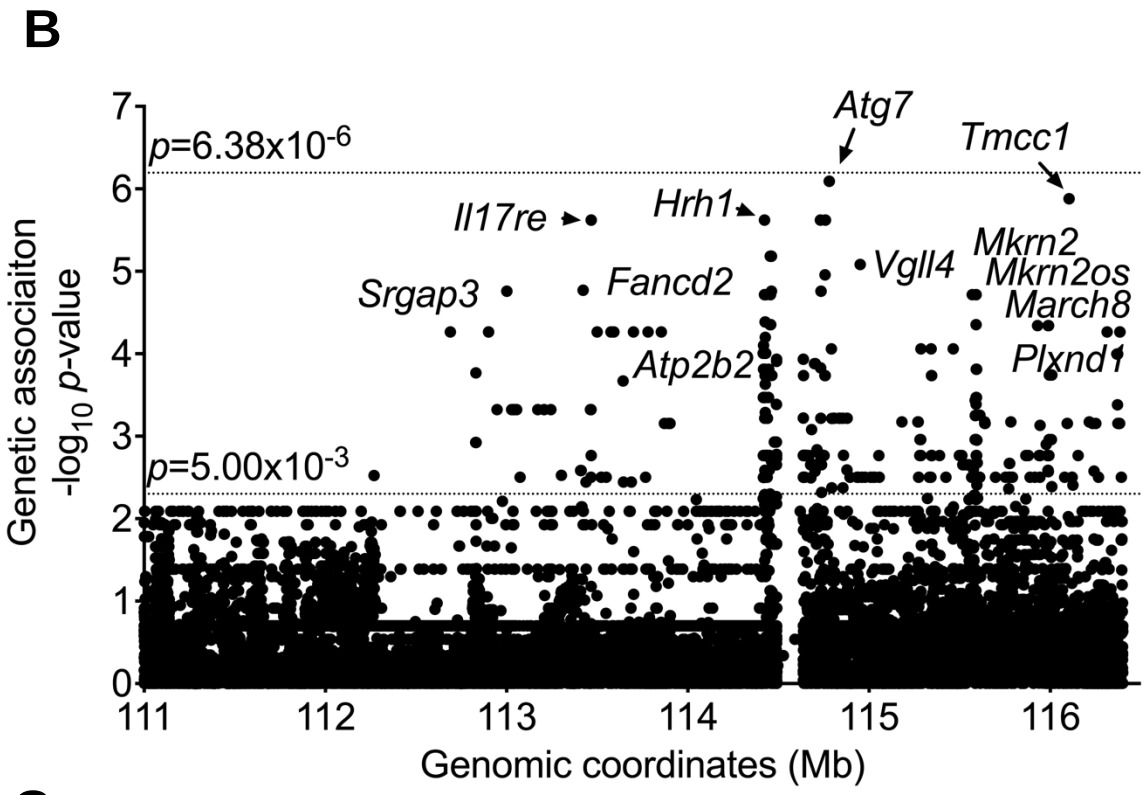

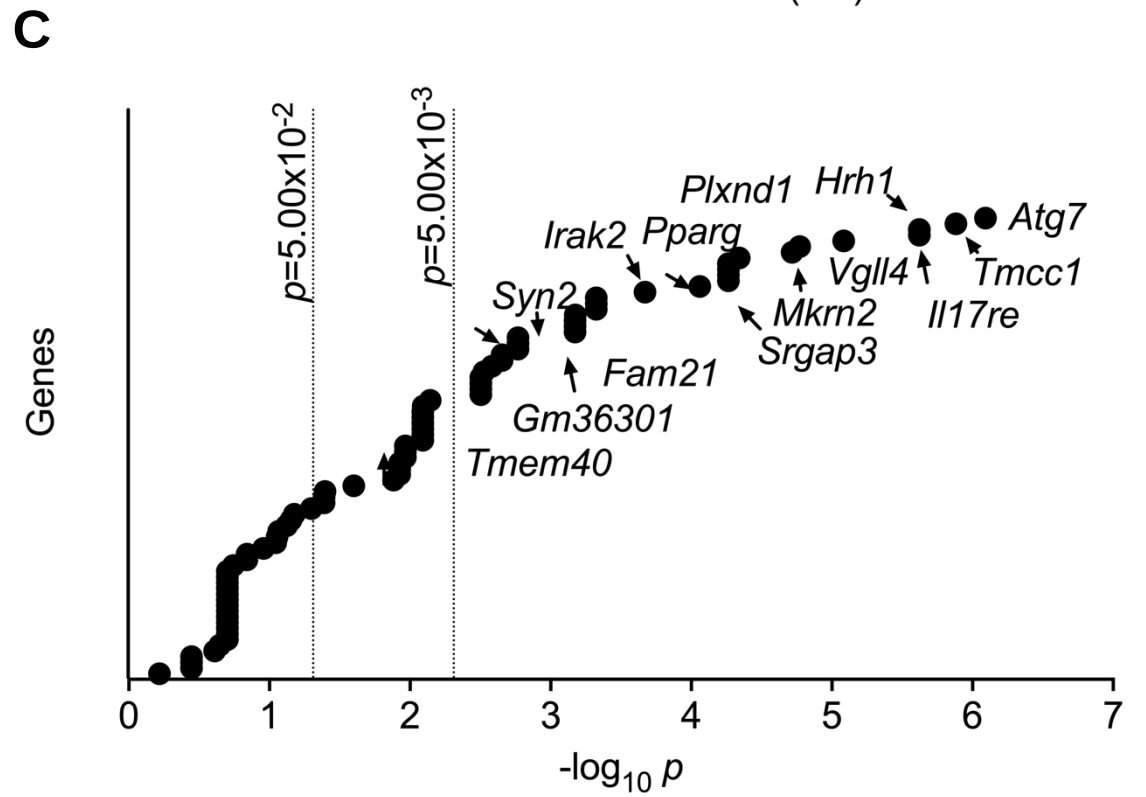

Figure 3. Integration of genetic and functional mapping approaches to predict candidates for *Bphse*. (**A**). The plot shows normalized negative log-transformed false positive rate of maximum functional enrichment (-log$_{10}$ *FPR*) on the y-axis. The x-axis denotes the corresponding normalized negative log-transformed genetic association scores. Candidates that were common across both approaches are shown. (**B**) The list of gene candidates as predicted by both genetic and functional approaches are ranked using a final gene score (S_{cg}) on x-axis and the gene names of top 20 candidates listed on y-axis. *Bphs*/*Hrh1* association is shown in red bar.

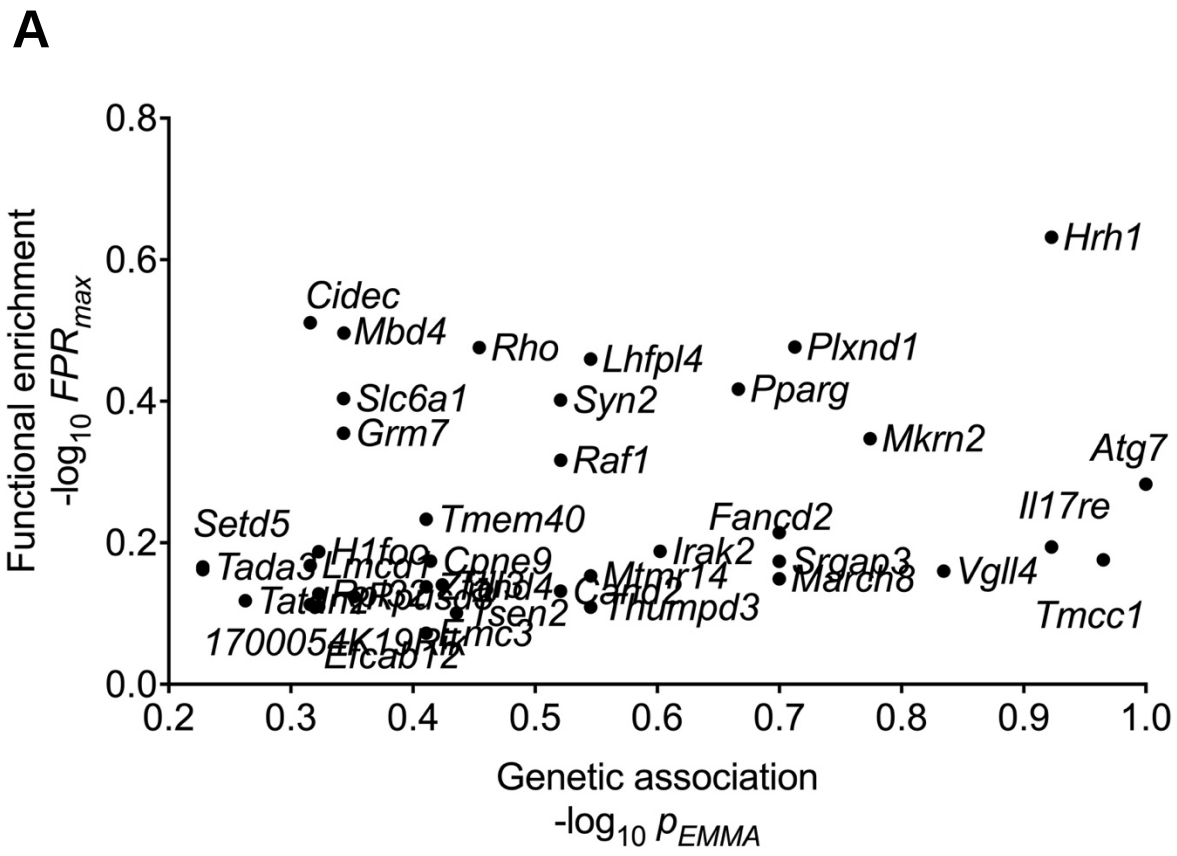

B

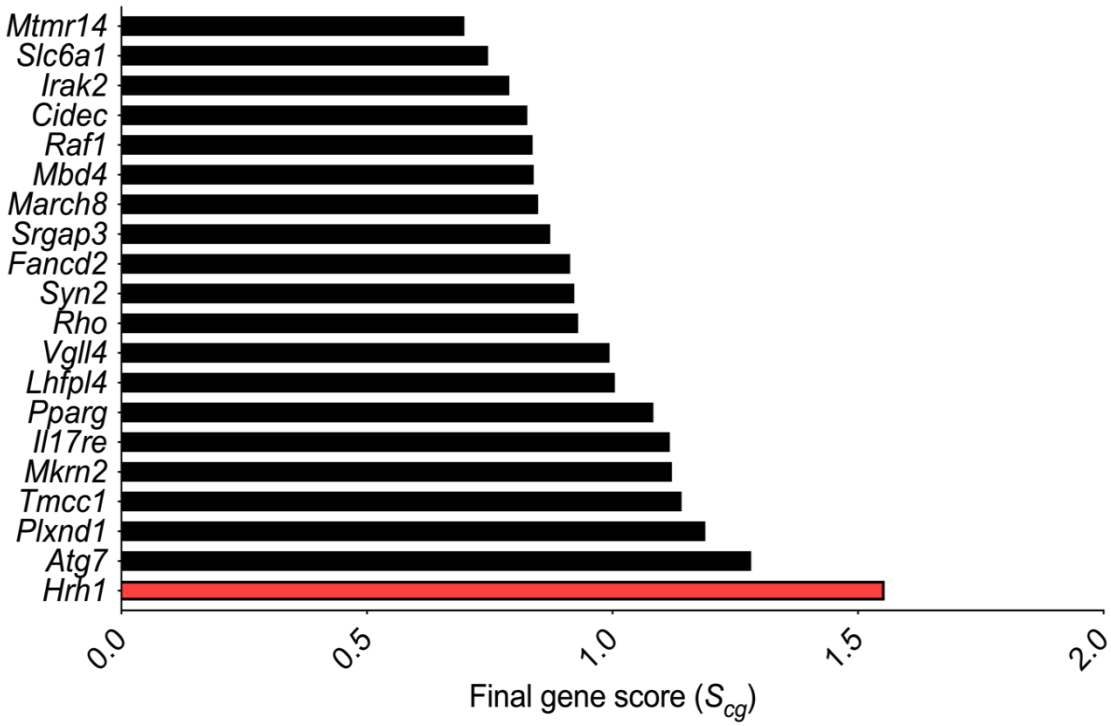

Supplementary Table 1. List of 50 inbred mouse strains used in genetic association testing.

Bphs Susceptible (41)				Bphs Resistant (9)
129S1/SvImJ	C57BL/6J	LP/J	PL/J	AKR/J
129T2/SvEmsJ	C57BLKS/J	MA/MyJ	PWD/PhJ	C3H/HeJ
129X1/SvJ	C57BR/cdJ	MOLD/RkJ	PWK/PhJ	CAST/EiJ
A/J	C57L/J	MOLF/EiJ	RF/J	CBA/J
A/WySnJ	C58/J	NOD/ShiLtJ	RIIIS/J	I/LnJ
BALB/cJ	CZECHII/EiJ	NON/ShiLtJ	SJL/J	MRL/MpJ
BALB/cByJ	DBA/1J	NOR/LtJ	SM/J	MSM/MsJ
BPL/1J	DBA/2J	NU/J	SWR/J	SF/CamEiJ
C57BL/10J	FVB/NJ	NZB/BlNJ		SKIVE/EiJ
C57BL/10ScNJ	JF1/MsJ	NZW/LacJ		
C57BL/6ByJ	LG/J	P/J		

Supplementary Table 2. Genetic association analysis identifies variants on Chr6 associated with Bphs[s].

Chr	bp (mm10)	SNP	Gene	*p*-value$_{EMMA}$
6	114780885	rs31440528	*I:Atg7*	8.10E-07
6	114732069	rs31439505	*I:Atg7*	2.39E-06
6	114758979	rs31445205	*I:Atg7*	2.39E-06
Suggestive SNPs (p<0.05)				
6	110966239	rs30498521	*I:Grm7*	1.07E-03
6	113466213	rs37366170	*I:Il17re*	3.14E-03
6	113521759	rs36681994	*I:Emc3*	3.14E-03
6	113766702	rs36921136	*I:Atp2b2*	3.14E-03
6	114427899	rs46432555	*I:Hrh1*	6.32E-05
6	114792207	rs31444358	*I:Atg7*	8.71E-05
6	114941577	rs6248634	*NC:LOC105242742*	3.14E-03
6	114951759	rs31456818	*Vgll4*	8.25E-06
6	115008370	rs6262329	*I:Tamm41*	3.14E-03
6	115181005	rs31473897	*I:Syn2*	6.72E-04
6	115286744	rs31484360	*NA*	8.71E-05
6	115321034	rs31484653	*NC:LOC105242744*	1.31E-02
6	115464239	rs51526492	*I:Pparg*	8.71E-05
6	115565855	rs51720018	*I:Tsen2*	3.14E-03
6	115612395	rs31487271	*I:Mkrn2*	5.54E-04
6	115663927	rs31496654	*I:Raf1*	2.79E-02
6	115753510	rs6160517	*I:Tmem40*	3.14E-03
6	115782690	rs31504457	*I:Cand2*	6.72E-04
6	115853377	rs31503770	*U5:Mbd4*	8.08E-03
6	115879245	rs31507517	*I:Ift122*	1.71E-03
6	115976241	rs31518615	*I:Plxnd1*	2.11E-02
6	116120070	rs31525210	*I:Tmcc1*	3.14E-03
6	116214868	rs31533291	*I:Fam21*	6.72E-04
6	116311087	rs31535245	*I:Zfand4*	1.08E-02
6	116402580	rs31537093	*I:March8*	6.72E-04
6	118643222	rs31587804	*I:Cacna1c*	1.32E-02
6	119353404	rs13472337	*U3:Adipor2*	3.86E-02

This list was generated using a stringent cut-off (*p<3.81E-06*) and a moderate cut-off (*p<5.00E-02*) using Efficient Mixed Model Association (EMMA). Only the most significant SNP tagging a gene is shown. The functional location of variants is listed using the following notation: intronic (I), synonymous change (Cs), 3' untranslated region variant (U3), 5' untranslated region variant (U5), not characterized (NC) and no gene (NA).

Supplementary Table 3. List of genetic variants identified ($p \leq 0.05$) using imputed genotypes across Chr6:111.0-116.5 Mb.

Chr	bp (mm10)	SNP	Gene	*p*-value$_{EMMA}$
6	111003149	rs223699795	*I:Grm7*	8.12E-03
6	112212190	rs37480964	*NC:1700054K19Rik*	1.19E-02
6	112309173	rs232269259	*I:Lmcd1*	1.19E-02
6	112900380	rs39644268	*I:Srgap3*	5.45E-05
6	113055745	rs217254661	*Cn:Thumpd3*	4.75E-04
6	113114553	rs262517352	*I:Setd5*	4.09E-02
6	113171903	rs38534902	*Cs:Lhfpl4*	4.75E-04
6	113244289	rs219248113	*I:Mtmr14*	4.75E-04
6	113302495	rs246910229	*I:Cpne9*	2.99E-03
6	113366827	rs236692255	*U3:Tada3*	4.09E-02
6	113408719	rs251474270	*I:Ttll3*	2.61E-03
6	113416087	rs37807004	*I:Rpusd3*	7.19E-03
6	113422346	rs214422450	*NA*	1.70E-05
6	113434320	rs240625517	*I:Cidec*	1.19E-02
6	113466530	rs36373609	*I:Il17re*	2.39E-06
6	113521759	rs36681994	*I:Emc3*	3.14E-03
6	113575822	rs225851814	*I:Fancd2*	5.45E-05
6	113643111	rs578496862	*I:Irak2*	2.14E-04
6	113701102	rs217976133	*I:Tatdn2*	2.51E-02
6	113780687	rs37734530	*I:Atp2b2*	5.45E-05
6	114046481	rs583881076	*I:Gm15083*	8.12E-03
6	114134236	rs227411521	*I:Slc6a1*	8.12E-03
6	114370888	rs579728563	*LOC105242741*	8.12E-03
6	114423235	rs46923527	*I:Hrh1*	2.39E-06
6	114780885	rs31440528	*I:Atg7*	8.10E-07
6	114951759	rs31456818	*I:Vgll4*	8.25E-06
6	115008370	rs6262329	*NC:Tamm41*	3.14E-03
6	115062105	rs586311125	*Gm36190*	8.12E-03
6	115134140	rs261281000	*I:Gm17733*	8.12E-03
6	115181005	rs31473897	*I:Syn2*	6.72E-04
6	115310919	rs31485016	*LOC105242743*	4.03E-02
6	115321034	rs31484653	*LOC105242744*	1.31E-02
6	115464239	rs51526492	*I:Pparg*	8.71E-05
6	115511777	rs46370506	*Gm36301*	1.71E-03
6	115533127	rs261206240	*I:Gm36355*	2.22E-03
6	115545283	rs212720020	*I:Tsen2*	2.22E-03
6	115591207	rs586340907	*I:Mkrn2*	1.92E-05
6	115638313	rs31494668	*Cs:Raf1*	6.70E-04
6	115753510	rs6160517	*I:Tmem40*	3.14E-03

6	115782690	rs31504457	*I:Cand2*	6.72E-04
6	115808296	rs224376952	*U5:Rpl32*	1.08E-02
6	115811422	rs249935404	*I:Efcab12*	1.08E-02
6	115853377	rs31503770	*U5:Mbd4*	8.08E-03
6	115865708	rs582751726	*I:Ift122*	1.71E-03
6	115938833	rs31509385	*U3:Rho*	1.71E-03
6	115944960	rs31515230	*U5:H1foo*	1.08E-02
6	115988747	rs31519252	*I:Plxnd1*	4.56E-05
6	116104121	rs235864765	*I:Tmcc1*	1.32E-06
6	116214868	rs31533291	*I:Fam21*	6.72E-04
6	116266396	rs31533962	*I:Zfand4*	3.14E-03
6	116383638	rs31534014	*I:March8*	5.45E-05

This list was generated using a moderate cut-off (*p<5.00E-02*) using Efficient Mixed Model Association (EMMA). Only the most significant SNP tagging a gene is listed. The functional location of variants is listed using the following notation: intronic (I), synonymous change (Cs), nonsynonymous change (Cn), 3' untranslated region variant (U3), 5' untranslated region variant (U5), not characterized (NC) and no gene (NA).

Supplementary Table 4. List of genes predicted to be functionally associated with Bphs physiological processes ranked by negative log of false positive rate.

Gene	Cardiac	ER/EMC/ERAD	GPCR	Histamine	PTX	T1H	VP	-log max FPR
C3ar1	1.38	1.22	1.32	1.71	1.56	2.89	2.36	2.89
Plxna1	1.10	2.24	0.64	0.43	0.60	1.03	0.53	2.24
Tnfrsf1a	1.35	1.35	1.22	1.07	1.33	2.08	1.18	2.08
Ret	1.81	2.03	1.04	1.06	1.17	0.88	1.20	2.03
Tgfa	1.25	2.03	0.88	0.90	0.87	1.01	1.09	2.03
Aqp1	1.89	1.43	0.90	0.85	0.81	1.21	1.11	1.89
Hrh1	1.01	1.83	0.72	0.70	0.92	0.67	0.69	1.83
Kcna1	1.65	1.81	1.70	0.94	1.06	0.86	0.93	1.81
Wnt7a	0.93	1.81	0.68	0.69	0.78	1.20	0.49	1.81
Emx1	1.17	1.79	1.37	1.06	1.51	0.98	0.94	1.79
Pex5	1.40	1.73	0.71	0.69	0.91	0.97	1.00	1.73
Npy	1.11	1.70	0.70	0.53	0.87	0.77	0.49	1.70
Ptpn6	0.93	1.24	1.24	1.02	1.28	1.67	1.24	1.67
Ogg1	0.85	1.66	0.41	0.45	0.53	0.75	0.45	1.66
Clec4e	0.62	0.84	0.85	0.67	0.81	1.64	0.67	1.64
Fgf23	0.88	1.12	1.40	1.43	1.03	1.07	1.63	1.63
Atp2b2	0.97	1.58	0.90	0.57	0.64	0.38	0.50	1.58
Ghrhr	1.07	1.52	1.58	0.94	1.13	0.94	0.94	1.58
Apobec1	0.59	1.49	0.56	0.67	0.85	1.57	0.82	1.57
Hoxa3	0.95	1.42	1.08	0.96	1.13	1.18	1.57	1.57
Cxcl12	1.57	1.26	0.70	0.61	0.91	0.90	0.80	1.57
Nr2c2	1.33	1.56	0.76	1.39	0.87	0.86	0.74	1.56
Gata2	1.13	1.55	0.84	0.69	0.93	0.95	0.75	1.55
Snca	1.41	1.54	1.49	1.24	1.23	0.79	1.20	1.54
Cacna1c	1.43	1.27	1.54	1.12	0.71	0.65	0.77	1.54
Mitf	1.20	1.53	1.48	1.00	1.00	1.23	1.07	1.53
Cd4	1.14	1.13	1.19	1.53	1.40	1.37	0.96	1.53
Hoxa13	1.33	1.53	1.27	0.99	1.09	1.22	1.00	1.53
Slc2a3	0.81	1.52	0.68	0.46	0.79	1.09	0.54	1.52
Dok1	0.70	1.52	0.58	0.75	0.74	1.28	0.71	1.52
Vhl	1.30	1.50	1.13	0.94	1.19	1.38	1.13	1.50
Il17ra	0.59	1.50	0.58	0.73	0.83	1.34	0.52	1.50
Kcna5	1.49	1.00	0.65	0.71	0.70	0.72	0.61	1.49
Clec4d	0.43	0.85	0.55	0.74	0.82	1.49	0.60	1.49

Adcyap1r1	1.41	1.48	0.87	0.58	0.80	0.80	0.53	1.48
Hoxa1	1.03	1.48	0.89	0.90	0.81	0.98	0.89	1.48
Cidec	1.48	0.85	0.83	0.75	0.78	1.00	0.53	1.48
Aicda	0.64	0.76	1.47	0.92	0.66	0.63	0.67	1.47
Bid	0.91	0.95	0.81	1.47	1.06	0.79	0.87	1.47
Il12rb2	0.85	0.68	1.40	1.46	0.99	1.01	0.90	1.46
Hoxa2	1.32	1.45	0.71	1.07	0.96	0.94	1.09	1.45
Mbd4	0.53	1.44	0.82	0.51	0.69	0.64	0.53	1.44
Tlx2	0.94	1.42	0.51	0.68	0.66	0.76	0.47	1.42
Ntf3	1.36	1.39	0.88	0.74	0.96	0.78	0.67	1.39
Cav3	1.39	0.85	0.59	0.45	0.70	0.81	0.52	1.39
Sftpb	0.83	1.38	0.51	0.55	0.58	0.95	0.48	1.38
Plxnd1	1.16	1.38	0.63	0.46	0.94	0.83	1.00	1.38
Rho	0.93	1.38	1.30	0.89	0.90	0.89	0.70	1.38
Hoxa9	0.80	1.35	1.04	0.77	0.71	0.75	0.64	1.35
Kcmf1	0.61	1.35	0.37	0.41	0.23	0.51	0.28	1.35
Ptms	0.94	1.35	0.28	0.13	0.22	0.67	0.34	1.35
Lhfpl4	0.45	1.33	0.37	0.24	0.33	0.45	0.31	1.33
Tacr1	1.18	1.28	1.33	1.06	1.25	1.08	0.87	1.33
Hoxa4	0.74	1.32	0.83	0.46	0.63	0.52	0.44	1.32
Hoxa11	0.97	1.31	0.88	0.83	0.60	0.96	0.71	1.31
Cd8a	0.80	0.75	1.01	0.97	1.14	1.29	0.66	1.29
Mgll	1.10	1.29	0.58	0.71	0.54	0.64	0.55	1.29
Abtb1	0.31	1.28	0.22	0.12	0.22	0.25	0.30	1.28
Crhr2	1.26	1.27	1.05	0.73	0.90	0.64	0.65	1.27
Add2	0.97	1.05	1.25	1.05	0.98	0.72	0.96	1.25
Mxd1	0.59	1.24	0.47	0.41	0.63	1.21	0.48	1.24
Iqsec1	0.36	1.24	0.34	0.27	0.26	0.39	0.13	1.24
Reg3g	0.46	0.32	0.78	0.62	0.78	1.24	0.45	1.24
Adamts9	0.47	1.22	0.53	0.44	0.62	0.71	0.51	1.22
Grid2	1.15	1.16	1.22	0.88	0.82	0.39	0.82	1.22
Asprv1	0.55	0.85	0.64	0.49	0.87	1.22	0.42	1.22
Tspan9	0.49	1.22	0.16	0.14	0.21	0.63	0.31	1.22
Oxtr	1.21	1.21	1.14	0.71	0.75	0.55	0.67	1.21
Cntn4	0.80	1.21	0.87	0.40	0.51	0.39	0.20	1.21
Pparg	1.14	0.95	1.21	1.05	0.82	0.78	1.08	1.21
Ltbr	0.72	1.00	0.32	0.35	0.50	1.21	0.62	1.21
Trh	0.74	1.20	0.62	0.59	0.58	0.72	0.41	1.20
Atoh1	1.15	0.73	1.20	1.19	1.00	1.18	0.82	1.20
Lrig1	0.45	1.19	0.42	0.33	0.42	0.43	0.41	1.19
Gdf3	0.90	0.88	0.77	0.73	0.80	1.19	0.57	1.19
Smyd1	1.17	1.03	0.72	0.55	0.58	0.52	0.65	1.17
Reg2	1.08	0.62	1.17	1.17	0.72	0.91	0.53	1.17

Slc6a1	0.74	1.17	0.70	0.42	0.69	0.31	0.42	1.17
Ctnna2	0.74	1.17	0.90	0.61	0.69	0.51	0.46	1.17
Syn2	0.77	1.16	0.87	0.49	0.53	0.68	0.31	1.16
Sspo	0.76	0.74	0.64	0.59	0.73	1.16	0.44	1.16
Ccnd2	0.96	1.15	0.59	0.76	0.85	1.07	0.63	1.15
C1s1	0.44	1.14	0.51	0.32	0.35	0.64	0.37	1.14
Rad52	0.51	1.14	0.46	0.46	0.53	0.42	0.46	1.14
Gp9	0.59	0.72	1.02	0.59	0.73	1.14	0.47	1.14
Dctn1	0.44	1.14	0.40	0.24	0.48	0.41	0.31	1.14
Atn1	0.83	1.13	0.64	0.46	0.47	0.54	0.43	1.13
H1fx	0.61	1.13	0.23	0.28	0.43	0.35	0.22	1.13
Vax2	1.11	1.00	0.78	0.90	0.72	0.93	0.49	1.11
Rmnd5a	0.29	1.11	0.18	0.15	0.44	0.25	0.09	1.11
Gpr27	0.96	1.09	0.71	0.42	0.59	0.60	0.41	1.09
Hoxa5	0.94	0.83	0.82	0.85	0.98	0.61	1.09	1.09
A2m	0.53	0.47	0.62	0.44	0.54	1.08	0.40	1.08
Cecr2	0.43	1.07	0.36	0.32	0.41	0.41	0.41	1.07
Prokr1	0.91	0.94	1.07	0.82	0.80	0.83	0.80	1.07
Zfp777	0.51	1.07	0.26	0.22	0.27	0.50	0.19	1.07
Ggcx	0.78	1.07	0.37	0.50	0.38	0.53	0.42	1.07
Tspan11	0.38	1.06	0.38	0.36	0.28	0.44	0.29	1.06
Rybp	0.73	1.06	0.45	0.34	0.41	0.72	0.37	1.06
Ift122	0.46	1.05	0.45	0.38	0.55	0.45	0.50	1.05
Usp18	0.93	0.67	0.48	0.59	0.88	1.05	0.51	1.05
Hpgds	0.84	0.65	1.05	0.90	1.01	0.83	0.80	1.05
Hoxa10	0.90	0.91	0.61	0.63	0.56	1.05	0.61	1.05
Foxp1	0.58	1.04	0.53	0.70	0.61	0.74	0.70	1.04
Slc6a6	0.84	1.03	0.45	0.40	0.55	0.58	0.53	1.03
Grm7	0.40	1.03	0.28	0.33	0.32	0.44	0.26	1.03
Figla	0.65	1.02	0.60	0.47	0.55	0.67	0.36	1.02
Fgf6	1.02	1.02	0.67	0.61	0.62	0.62	0.54	1.02
Podxl2	0.40	1.01	0.27	0.31	0.30	0.39	0.31	1.01
Cd163	0.19	0.31	1.01	0.31	0.37	0.34	0.29	1.01
Antxr1	0.59	0.79	1.01	0.56	0.84	0.68	0.77	1.01
Sema4f	0.57	1.01	0.81	0.40	0.56	0.37	0.37	1.01
Hoxa7	0.55	1.01	0.54	0.54	0.62	0.52	0.50	1.01
Cyp26b1	0.68	1.01	0.70	0.67	0.58	0.56	0.63	1.01
Ghrl	1.01	0.89	0.85	0.81	0.67	0.39	0.65	1.01
Mkrn2	0.59	1.00	0.28	0.39	0.29	0.35	0.27	1.00
Tuba8	0.82	1.00	0.32	0.34	0.42	0.51	0.32	1.00
Mfap5	0.78	0.56	0.43	0.42	0.40	0.99	0.42	0.99
Rtkn	0.36	0.98	0.24	0.30	0.42	0.35	0.38	0.98
Alms1	0.62	0.80	0.69	0.89	0.97	0.37	0.85	0.97

Hoxa6	0.35	0.97	0.37	0.24	0.32	0.45	0.26	0.97
Wnk1	0.57	0.96	0.33	0.41	0.39	0.64	0.43	0.96
Mpp6	0.18	0.96	0.23	0.21	0.28	0.25	0.15	0.96
Actg2	0.48	0.57	0.30	0.45	0.41	0.96	0.33	0.96
Gmcl1	0.35	0.96	0.31	0.28	0.24	0.38	0.30	0.96
Clstn3	0.45	0.96	0.29	0.30	0.24	0.29	0.38	0.96
Kcna6	0.78	0.95	0.93	0.50	0.64	0.50	0.50	0.95
Cntnap2	0.41	0.95	0.42	0.31	0.39	0.25	0.25	0.95
Bola3	0.36	0.95	0.35	0.16	0.08	0.31	0.20	0.95
Edem1	0.25	0.35	0.36	0.25	0.27	0.95	0.31	0.95
Pcgf1	0.18	0.94	0.22	0.19	0.19	0.24	0.20	0.94
Gimap5	0.56	0.94	0.57	0.53	0.55	0.65	0.62	0.94
Clec4n	0.34	0.47	0.42	0.53	0.68	0.94	0.81	0.94
Rnf103	0.21	0.94	0.28	0.28	0.29	0.43	0.34	0.94
Kdm5a	0.49	0.93	0.34	0.50	0.52	0.53	0.47	0.93
Evx1	0.58	0.41	0.93	0.64	0.57	0.55	0.44	0.93
Slc6a11	0.36	0.93	0.31	0.31	0.36	0.32	0.28	0.93
Timp4	0.58	0.92	0.44	0.34	0.34	0.46	0.40	0.92
Klf15	0.92	0.79	0.49	0.50	0.57	0.45	0.51	0.92
Dnajb8	0.68	0.62	0.92	0.53	0.63	0.62	0.55	0.92
Raf1	0.48	0.92	0.53	0.73	0.73	0.65	0.64	0.92
Itpr1	0.74	0.82	0.34	0.31	0.45	0.91	0.36	0.91
Tmem176a	0.47	0.60	0.26	0.27	0.46	0.91	0.36	0.91
Creb5	0.73	0.91	0.47	0.65	0.65	0.58	0.48	0.91
Egr4	0.59	0.91	0.45	0.42	0.41	0.60	0.42	0.91
Aoc1	0.63	0.84	0.55	0.42	0.72	0.91	0.46	0.91
Aldh1l1	0.57	0.90	0.29	0.32	0.21	0.51	0.29	0.90
Loxl3	0.45	0.90	0.56	0.38	0.45	0.61	0.36	0.90
Atp6v1b1	0.32	0.89	0.59	0.34	0.46	0.42	0.41	0.89
Slc6a13	0.50	0.89	0.33	0.34	0.40	0.48	0.29	0.89
Bhlhe40	0.83	0.60	0.42	0.44	0.47	0.89	0.47	0.89
Rarres2	0.71	0.88	0.49	0.34	0.31	0.53	0.39	0.88
Fbln2	0.69	0.43	0.44	0.36	0.44	0.88	0.47	0.88
Gpr162	0.58	0.88	0.56	0.38	0.48	0.64	0.34	0.88
Skap2	0.36	0.54	0.42	0.32	0.45	0.88	0.24	0.88
Il5ra	0.47	0.55	0.87	0.55	0.53	0.52	0.56	0.87
Reg3a	0.41	0.49	0.87	0.57	0.56	0.36	0.38	0.87
Aak1	0.51	0.87	0.55	0.39	0.47	0.24	0.32	0.87
C1ra	0.60	0.55	0.37	0.38	0.60	0.87	0.40	0.87
Reg1	0.51	0.55	0.86	0.65	0.54	0.60	0.43	0.86
Magi1	0.50	0.69	0.86	0.32	0.35	0.48	0.40	0.86
Bmp10	0.85	0.84	0.68	0.58	0.61	0.86	0.49	0.86
Gng12	0.25	0.33	0.30	0.30	0.16	0.86	0.29	0.86

P3h3	0.41	0.86	0.48	0.31	0.42	0.56	0.25	0.86
Mcm2	0.39	0.44	0.65	0.42	0.86	0.48	0.56	0.86
Clec4a2	0.41	0.57	0.47	0.69	0.60	0.86	0.46	0.86
Akap3	0.40	0.46	0.85	0.44	0.46	0.48	0.42	0.85
Vmn1r12	0.15	0.16	0.85	0.24	0.19	0.27	0.18	0.85
Wbp1	0.47	0.85	0.23	0.10	0.11	0.39	0.08	0.85
Stambp	0.54	0.85	0.34	0.34	0.42	0.43	0.38	0.85
Lag3	0.59	0.85	0.60	0.56	0.76	0.66	0.57	0.85
Grip2	0.38	0.85	0.46	0.40	0.35	0.41	0.42	0.85
Rab43	0.64	0.84	0.53	0.32	0.31	0.58	0.39	0.84
Capg	0.35	0.76	0.43	0.61	0.52	0.84	0.53	0.84
Zfp384	0.39	0.83	0.42	0.33	0.17	0.41	0.33	0.83
Rimklb	0.46	0.83	0.40	0.36	0.28	0.43	0.19	0.83
Nfe2l3	0.67	0.83	0.49	0.52	0.46	0.70	0.42	0.83
Eif2ak3	0.56	0.78	0.83	0.68	0.83	0.77	0.71	0.83
Cntn3	0.55	0.42	0.83	0.44	0.50	0.32	0.36	0.83
Atg7	0.58	0.82	0.64	0.46	0.56	0.62	0.56	0.82
Klrg1	0.55	0.82	0.71	0.55	0.55	0.64	0.39	0.82
Rasgef1a	0.42	0.80	0.76	0.28	0.28	0.48	0.15	0.80
Aup1	0.51	0.80	0.23	0.18	0.18	0.40	0.32	0.80
Nop2	0.27	0.39	0.18	0.27	0.16	0.80	0.19	0.80
Vwf	0.58	0.80	0.65	0.43	0.57	0.60	0.72	0.80
Dysf	0.67	0.67	0.43	0.38	0.40	0.80	0.44	0.80
Nat8f1	0.51	0.80	0.33	0.29	0.49	0.46	0.19	0.80
Prr15	0.44	0.79	0.61	0.36	0.50	0.64	0.33	0.79
Nanog	0.41	0.54	0.50	0.47	0.32	0.79	0.40	0.79
Reg3b	0.40	0.32	0.78	0.47	0.65	0.56	0.40	0.78
Gt(ROSA)26Sor	0.34	0.37	0.60	0.78	0.75	0.37	0.63	0.78
1700003E16Rik	0.36	0.78	0.27	0.25	0.13	0.40	0.25	0.78
Necap1	0.26	0.77	0.26	0.20	0.27	0.29	0.19	0.77
Tacstd2	0.42	0.37	0.44	0.39	0.55	0.77	0.34	0.77
Wipf3	0.39	0.77	0.32	0.32	0.44	0.40	0.21	0.77
Gadd45a	0.70	0.70	0.50	0.64	0.70	0.77	0.66	0.77
Neurod6	0.65	0.77	0.71	0.45	0.55	0.57	0.49	0.77
Mturn	0.56	0.77	0.49	0.34	0.43	0.65	0.34	0.77
Slc41a3	0.48	0.77	0.39	0.32	0.38	0.23	0.34	0.77
Gimap4	0.44	0.76	0.51	0.46	0.61	0.50	0.45	0.76
Gnb3	0.55	0.46	0.76	0.37	0.44	0.43	0.28	0.76
Repin1	0.42	0.76	0.30	0.25	0.30	0.42	0.15	0.76
Prok2	0.47	0.76	0.53	0.38	0.32	0.46	0.35	0.76
Erc1	0.40	0.76	0.38	0.33	0.18	0.41	0.26	0.76
Ano2	0.33	0.75	0.32	0.19	0.37	0.31	0.39	0.75
Arpc4	0.46	0.41	0.22	0.16	0.53	0.75	0.17	0.75

Hdhd5	0.44	0.74	0.63	0.45	0.44	0.15	0.41	0.74
Chn2	0.40	0.74	0.34	0.30	0.36	0.28	0.34	0.74
Zfp467	0.42	0.74	0.16	0.31	0.50	0.57	0.24	0.74
Retsat	0.54	0.73	0.31	0.29	0.17	0.41	0.26	0.73
Phc1	0.39	0.73	0.49	0.40	0.50	0.21	0.50	0.73
Dppa3	0.71	0.57	0.57	0.67	0.73	0.67	0.50	0.73
Gapdh	0.73	0.59	0.33	0.28	0.43	0.37	0.39	0.73
Mlf2	0.43	0.73	0.25	0.19	0.42	0.41	0.18	0.73
Mug1	0.52	0.73	0.43	0.62	0.71	0.62	0.47	0.73
Ezh2	0.31	0.59	0.23	0.36	0.72	0.32	0.36	0.72
Fxyd4	0.64	0.72	0.47	0.48	0.47	0.58	0.58	0.72
Scnn1a	0.65	0.72	0.66	0.57	0.47	0.51	0.57	0.72
Hnrnpa2b1	0.19	0.35	0.25	0.20	0.72	0.22	0.21	0.72
Vmn1r45	0.25	0.21	0.72	0.30	0.24	0.18	0.30	0.72
Cd8b1	0.46	0.65	0.43	0.43	0.59	0.72	0.49	0.72
Htra2	0.43	0.71	0.29	0.40	0.61	0.42	0.44	0.71
Cd9	0.33	0.60	0.28	0.34	0.24	0.71	0.45	0.71
Aplf	0.40	0.71	0.33	0.42	0.43	0.37	0.30	0.71
Noto	0.48	0.70	0.40	0.36	0.53	0.57	0.44	0.70
Cycs	0.43	0.70	0.26	0.64	0.70	0.25	0.41	0.70
Txnrd3	0.37	0.70	0.26	0.26	0.40	0.29	0.22	0.70
Pcbp1	0.18	0.21	0.18	0.22	0.69	0.20	0.19	0.69
C1rl	0.26	0.34	0.69	0.23	0.26	0.27	0.24	0.69
Mad2l1	0.24	0.46	0.19	0.32	0.69	0.28	0.31	0.69
Vmn2r26	0.47	0.69	0.51	0.46	0.46	0.48	0.36	0.69
Pde1c	0.38	0.68	0.52	0.29	0.37	0.17	0.30	0.68
Tmem121b	0.42	0.68	0.50	0.37	0.38	0.17	0.29	0.68
Adipor2	0.60	0.68	0.45	0.45	0.36	0.38	0.38	0.68
Atoh8	0.40	0.57	0.67	0.35	0.22	0.41	0.41	0.67
Tmem40	0.41	0.60	0.50	0.37	0.47	0.67	0.33	0.67
Vmn1r41	0.42	0.32	0.67	0.53	0.49	0.44	0.42	0.67
Elmod3	0.54	0.66	0.26	0.18	0.31	0.24	0.05	0.66
Tgoln1	0.38	0.66	0.27	0.32	0.36	0.55	0.21	0.66
Iffo1	0.33	0.66	0.34	0.33	0.07	0.28	0.21	0.66
Plekhg6	0.49	0.66	0.38	0.40	0.36	0.58	0.41	0.66
Sfxn5	0.37	0.66	0.32	0.32	0.21	0.32	0.19	0.66
Cd207	0.39	0.51	0.61	0.47	0.65	0.48	0.45	0.65
Emg1	0.18	0.65	0.18	0.24	0.50	0.22	0.19	0.65
Chd4	0.26	0.65	0.38	0.29	0.43	0.40	0.45	0.65
Rab11fip5	0.41	0.65	0.29	0.22	0.23	0.54	0.33	0.65
Lbx2	0.41	0.65	0.45	0.41	0.43	0.43	0.45	0.65
Fkbp9	0.29	0.18	0.28	0.15	0.45	0.65	0.25	0.65
1700063H04Rik	0.40	0.36	0.65	0.30	0.24	0.20	0.36	0.65

Snx10	0.33	0.24	0.25	0.29	0.46	0.65	0.26	0.65
Gpnmb	0.38	0.62	0.51	0.36	0.50	0.64	0.39	0.64
Tpra1	0.31	0.64	0.27	0.14	0.41	0.39	0.16	0.64
Wnt5b	0.46	0.64	0.38	0.36	0.30	0.57	0.28	0.64
Ccdc142	0.29	0.64	0.31	0.21	0.21	0.36	0.12	0.64
Rab7	0.26	0.37	0.32	0.21	0.45	0.64	0.19	0.64
Cd27	0.46	0.49	0.61	0.55	0.64	0.53	0.49	0.64
Usp5	0.47	0.63	0.32	0.25	0.09	0.41	0.14	0.63
Nod1	0.30	0.63	0.38	0.30	0.39	0.36	0.33	0.63
Fgd5	0.48	0.63	0.40	0.29	0.25	0.41	0.39	0.63
Mob1a	0.46	0.63	0.29	0.33	0.34	0.51	0.25	0.63
Fbxo41	0.44	0.63	0.30	0.24	0.42	0.41	0.25	0.63
Mrpl53	0.19	0.63	0.26	0.17	0.22	0.24	0.15	0.63
Uroc1	0.48	0.63	0.46	0.36	0.33	0.46	0.36	0.63
Copg1	0.23	0.30	0.18	0.23	0.33	0.62	0.23	0.62
Zfp9	0.30	0.62	0.40	0.26	0.29	0.34	0.21	0.62
Nap1l5	0.38	0.62	0.43	0.27	0.27	0.27	0.29	0.62
Chl1	0.39	0.45	0.48	0.41	0.62	0.43	0.38	0.62
Slc6a12	0.62	0.51	0.58	0.41	0.42	0.41	0.39	0.62
Iqsec3	0.22	0.40	0.62	0.32	0.34	0.18	0.15	0.62
Fancd2	0.53	0.56	0.43	0.50	0.62	0.29	0.45	0.62
Hdac11	0.31	0.62	0.27	0.15	0.26	0.18	0.29	0.62
Rassf4	0.38	0.62	0.40	0.28	0.28	0.60	0.29	0.62
Vmn1r47	0.36	0.35	0.62	0.40	0.52	0.44	0.42	0.62
Ninj2	0.54	0.52	0.45	0.36	0.43	0.62	0.32	0.62
Washc2	0.25	0.61	0.28	0.18	0.25	0.40	0.16	0.61
Parp11	0.30	0.61	0.37	0.25	0.28	0.31	0.30	0.61
Tmem176b	0.40	0.48	0.29	0.54	0.35	0.61	0.33	0.61
Lrrc23	0.55	0.43	0.43	0.41	0.46	0.61	0.44	0.61
Vopp1	0.22	0.61	0.50	0.35	0.20	0.37	0.36	0.61
Tex261	0.30	0.61	0.24	0.21	0.13	0.35	0.28	0.61
Tuba3a	0.29	0.60	0.24	0.27	0.26	0.49	0.23	0.60
Vmn1r42	0.35	0.29	0.60	0.43	0.36	0.35	0.35	0.60
Tril	0.41	0.60	0.42	0.28	0.41	0.48	0.33	0.60
Eno2	0.35	0.60	0.33	0.29	0.42	0.38	0.40	0.60
Ino80b	0.32	0.60	0.33	0.23	0.08	0.35	0.17	0.60
Immt	0.32	0.60	0.18	0.28	0.28	0.35	0.15	0.60
Smyd5	0.21	0.60	0.50	0.14	0.30	0.35	0.18	0.60
Fbxl14	0.24	0.29	0.18	0.33	0.23	0.59	0.17	0.59
Alox5	0.41	0.47	0.51	0.48	0.59	0.58	0.49	0.59
Tapbpl	0.44	0.59	0.51	0.32	0.45	0.51	0.28	0.59
Gkn1	0.24	0.57	0.59	0.34	0.43	0.34	0.23	0.59
Prickle2	0.37	0.59	0.35	0.28	0.37	0.30	0.25	0.59

Cacna2d4	0.26	0.58	0.35	0.24	0.22	0.25	0.35	0.58
Atp6v0e2	0.30	0.58	0.30	0.20	0.36	0.22	0.21	0.58
Ankrd26	0.47	0.48	0.56	0.58	0.54	0.35	0.51	0.58
Fam221a	0.18	0.39	0.58	0.15	0.12	0.18	0.20	0.58
Creld1	0.33	0.58	0.29	0.14	0.26	0.33	0.16	0.58
Vamp1	0.38	0.58	0.37	0.35	0.41	0.55	0.34	0.58
Cntn6	0.37	0.58	0.52	0.43	0.33	0.32	0.33	0.58
4921507P07Rik	0.40	0.58	0.25	0.25	0.09	0.43	0.30	0.58
Krcc1	0.22	0.57	0.19	0.20	0.17	0.29	0.09	0.57
Dqx1	0.36	0.53	0.57	0.27	0.36	0.35	0.29	0.57
Acrbp	0.28	0.57	0.48	0.30	0.46	0.31	0.25	0.57
Pole4	0.15	0.25	0.24	0.24	0.57	0.17	0.20	0.57
St3gal5	0.36	0.57	0.31	0.33	0.22	0.28	0.22	0.57
Tet3	0.36	0.57	0.36	0.31	0.19	0.38	0.14	0.57
Vmn1r20	0.16	0.23	0.57	0.20	0.14	0.21	0.21	0.57
Vmn1r25	0.24	0.24	0.57	0.38	0.42	0.46	0.34	0.57
Ing4	0.41	0.57	0.39	0.31	0.44	0.44	0.29	0.57
Gkn2	0.35	0.38	0.56	0.42	0.45	0.43	0.37	0.56
Hoxa11os	0.55	0.39	0.38	0.39	0.56	0.44	0.39	0.56
Vmn1r27	0.10	0.27	0.56	0.28	0.18	0.15	0.22	0.56
Tcf7l1	0.40	0.56	0.43	0.43	0.48	0.30	0.49	0.56
Il17re	0.40	0.56	0.47	0.39	0.32	0.45	0.42	0.56
Spsb2	0.46	0.56	0.39	0.33	0.29	0.42	0.43	0.56
Vmn1r15	0.43	0.37	0.54	0.39	0.56	0.37	0.35	0.56
Vmn1r26	0.21	0.25	0.56	0.26	0.14	0.15	0.28	0.56
Anxa4	0.31	0.35	0.32	0.26	0.19	0.56	0.32	0.56
Mrpl51	0.31	0.56	0.45	0.28	0.10	0.28	0.14	0.56
Lrrn1	0.43	0.55	0.55	0.36	0.43	0.47	0.31	0.55
Gfpt1	0.44	0.44	0.48	0.35	0.17	0.55	0.33	0.55
Arl8b	0.24	0.34	0.55	0.21	0.18	0.41	0.29	0.55
Zxdc	0.43	0.55	0.49	0.27	0.21	0.44	0.23	0.55
Fabp1	0.55	0.46	0.44	0.43	0.51	0.52	0.40	0.55
Reg3d	0.23	0.32	0.55	0.44	0.45	0.49	0.42	0.55
Vmn1r46	0.32	0.32	0.55	0.42	0.46	0.40	0.39	0.55
Frmd4b	0.34	0.50	0.46	0.25	0.23	0.55	0.35	0.55
Fam136a	0.13	0.25	0.22	0.30	0.54	0.20	0.19	0.54
Irak2	0.27	0.54	0.35	0.21	0.31	0.39	0.24	0.54
H1foo	0.45	0.54	0.39	0.36	0.40	0.47	0.23	0.54
Zfp239	0.31	0.32	0.54	0.32	0.40	0.16	0.33	0.54
Mmrn1	0.27	0.26	0.54	0.32	0.38	0.37	0.43	0.54
Efcc1	0.38	0.36	0.54	0.36	0.19	0.41	0.31	0.54
Mthfd2	0.26	0.47	0.26	0.46	0.45	0.54	0.30	0.54
Ndnf	0.25	0.35	0.53	0.26	0.40	0.30	0.29	0.53

Npvf	0.28	0.30	0.53	0.43	0.44	0.24	0.35	0.53
Olfr215	0.26	0.53	0.32	0.31	0.20	0.32	0.23	0.53
Krba1	0.24	0.53	0.16	0.20	0.27	0.14	0.24	0.53
Tmem150a	0.48	0.53	0.27	0.28	0.40	0.35	0.26	0.53
Cbx3	0.30	0.53	0.24	0.31	0.27	0.45	0.33	0.53
Fam13a	0.52	0.38	0.37	0.23	0.20	0.45	0.35	0.52
Prmt8	0.40	0.52	0.36	0.29	0.29	0.42	0.17	0.52
Pianp	0.26	0.40	0.52	0.32	0.30	0.22	0.25	0.52
Clec4f	0.50	0.49	0.41	0.44	0.43	0.52	0.33	0.52
Kbtbd12	0.37	0.35	0.52	0.38	0.45	0.24	0.37	0.52
Clec4a3	0.32	0.43	0.52	0.34	0.37	0.33	0.32	0.52
Abcg2	0.25	0.31	0.36	0.52	0.38	0.32	0.32	0.52
Spr	0.47	0.51	0.29	0.16	0.24	0.29	0.18	0.51
Foxj2	0.37	0.51	0.40	0.26	0.44	0.39	0.41	0.51
Ppp1r17	0.43	0.40	0.51	0.32	0.42	0.34	0.34	0.51
Vmn1r40	0.32	0.30	0.51	0.38	0.45	0.45	0.33	0.51
Ptcd3	0.19	0.34	0.46	0.51	0.51	0.17	0.08	0.51
Il17rc	0.51	0.50	0.32	0.27	0.45	0.36	0.36	0.51
M1ap	0.36	0.51	0.39	0.37	0.36	0.38	0.44	0.51
Gimap9	0.30	0.43	0.51	0.31	0.34	0.37	0.27	0.51
BC048671	0.22	0.38	0.51	0.35	0.38	0.22	0.42	0.51
Inmt	0.49	0.50	0.49	0.41	0.42	0.51	0.38	0.51
Gm5111	0.36	0.49	0.32	0.26	0.42	0.51	0.23	0.51
Tmcc1	0.30	0.51	0.27	0.15	0.35	0.36	0.22	0.51
Chst13	0.33	0.35	0.51	0.33	0.27	0.41	0.14	0.51
Arhgap25	0.27	0.29	0.51	0.35	0.43	0.28	0.42	0.51
Sec61a1	0.35	0.51	0.27	0.36	0.33	0.50	0.43	0.51
Cnbp	0.18	0.23	0.18	0.22	0.51	0.20	0.23	0.51
Cul1	0.23	0.37	0.18	0.21	0.50	0.21	0.28	0.50
Cpne9	0.33	0.50	0.42	0.28	0.40	0.46	0.32	0.50
Srgap3	0.40	0.50	0.40	0.34	0.34	0.33	0.27	0.50
Vamp8	0.37	0.44	0.31	0.29	0.34	0.50	0.38	0.50
Zfp956	0.21	0.50	0.43	0.23	0.15	0.34	0.22	0.50
Eva1a	0.45	0.50	0.36	0.33	0.20	0.45	0.14	0.50
Cfap100	0.39	0.50	0.38	0.07	0.23	0.43	0.26	0.50
Tpi1	0.43	0.50	0.18	0.13	0.27	0.31	0.21	0.50
Ankrd53	0.23	0.50	0.41	0.19	0.28	0.32	0.25	0.50
Smarcad1	0.50	0.43	0.47	0.46	0.41	0.21	0.48	0.50
Kdm3a	0.33	0.39	0.38	0.50	0.28	0.32	0.40	0.50
Csgalnact2	0.23	0.49	0.22	0.20	0.22	0.24	0.21	0.49
Gimap7	0.35	0.43	0.49	0.38	0.47	0.42	0.38	0.49
Cops7a	0.20	0.49	0.22	0.21	0.29	0.29	0.14	0.49
Tmem43	0.44	0.39	0.31	0.31	0.28	0.49	0.20	0.49

Pdia4	0.23	0.49	0.27	0.22	0.19	0.25	0.15	0.49
Tra2a	0.27	0.49	0.21	0.16	0.23	0.27	0.35	0.49
Gsdme	0.36	0.49	0.35	0.31	0.39	0.37	0.36	0.49
Serbp1	0.18	0.48	0.18	0.24	0.34	0.49	0.26	0.49
Lmcd1	0.33	0.38	0.49	0.35	0.09	0.37	0.35	0.49
Tmf1	0.31	0.48	0.26	0.20	0.13	0.25	0.28	0.48
Vmn1r29	0.26	0.36	0.43	0.33	0.48	0.21	0.36	0.48
Mical3	0.34	0.48	0.43	0.17	0.21	0.42	0.31	0.48
Vmn1r49	0.29	0.48	0.40	0.35	0.36	0.39	0.33	0.48
M6pr	0.37	0.38	0.27	0.48	0.48	0.41	0.43	0.48
Tada3	0.30	0.48	0.34	0.29	0.14	0.45	0.14	0.48
Exoc6b	0.22	0.48	0.31	0.28	0.28	0.43	0.35	0.48
Gars	0.18	0.23	0.20	0.19	0.48	0.30	0.19	0.48
Vmn1r13	0.26	0.31	0.47	0.43	0.48	0.33	0.46	0.48
Brk1	0.18	0.22	0.26	0.18	0.48	0.24	0.21	0.48
Lsm3	0.15	0.48	0.24	0.17	0.17	0.18	0.25	0.48
Vmn1r44	0.37	0.35	0.48	0.42	0.45	0.46	0.40	0.48
Depp1	0.35	0.39	0.48	0.28	0.26	0.27	0.32	0.48
Atp6v1e1	0.29	0.34	0.48	0.23	0.32	0.33	0.20	0.48
Scrn1	0.42	0.47	0.25	0.26	0.34	0.38	0.21	0.47
Eif4e3	0.47	0.44	0.36	0.19	0.38	0.40	0.22	0.47
Vamp5	0.39	0.44	0.47	0.22	0.33	0.16	0.20	0.47
Vmn1r14	0.24	0.27	0.47	0.38	0.42	0.14	0.43	0.47
Nup210	0.32	0.39	0.47	0.24	0.14	0.33	0.25	0.47
Nat8f2	0.22	0.31	0.47	0.36	0.39	0.34	0.32	0.47
Vmn1r7	0.25	0.47	0.30	0.28	0.28	0.29	0.15	0.47
Setd5	0.36	0.47	0.42	0.16	0.26	0.42	0.15	0.47
Igf2bp3	0.37	0.35	0.47	0.34	0.41	0.44	0.30	0.47
Ppp4r2	0.33	0.39	0.30	0.26	0.19	0.47	0.28	0.47
Mrps25	0.14	0.19	0.21	0.24	0.47	0.11	0.11	0.47
Vgll4	0.44	0.46	0.40	0.35	0.28	0.07	0.40	0.46
Tax1bp1	0.25	0.46	0.45	0.38	0.39	0.32	0.41	0.46
4931417E11Rik	0.34	0.39	0.46	0.36	0.37	0.24	0.44	0.46
Lrrtm1	0.37	0.46	0.44	0.40	0.29	0.23	0.37	0.46
Olfr212	0.16	0.23	0.46	0.26	0.25	0.38	0.26	0.46
Cct7	0.18	0.20	0.18	0.18	0.46	0.20	0.19	0.46
Avl9	0.25	0.46	0.28	0.32	0.15	0.20	0.19	0.46
Vmn1r10	0.21	0.35	0.46	0.39	0.43	0.09	0.41	0.46
Sumf1	0.29	0.35	0.29	0.46	0.43	0.38	0.42	0.46
Osbpl3	0.36	0.42	0.17	0.19	0.27	0.46	0.11	0.46
Slc4a5	0.35	0.43	0.36	0.31	0.39	0.45	0.19	0.45
Brpf1	0.16	0.43	0.19	0.11	0.14	0.45	0.12	0.45
Chchd6	0.14	0.38	0.45	0.24	0.28	0.23	0.08	0.45

Dguok	0.21	0.21	0.35	0.26	0.18	0.45	0.17	0.45
1810044D09Rik	0.45	0.41	0.44	0.36	0.28	0.27	0.34	0.45
Lrtm2	0.32	0.45	0.42	0.31	0.19	0.07	0.25	0.45
Nat8	0.44	0.38	0.34	0.36	0.21	0.34	0.42	0.44
Lrrc61	0.37	0.44	0.33	0.27	0.16	0.29	0.25	0.44
Lancl2	0.27	0.32	0.23	0.24	0.44	0.14	0.21	0.44
Mtmr14	0.30	0.44	0.30	0.29	0.14	0.28	0.34	0.44
Arl6ip5	0.18	0.32	0.42	0.18	0.32	0.44	0.19	0.44
Tmsb10	0.26	0.33	0.33	0.18	0.44	0.42	0.29	0.44
Nat8f4	0.25	0.44	0.32	0.34	0.22	0.28	0.33	0.44
4930544G11Rik	0.33	0.35	0.25	0.25	0.27	0.44	0.25	0.44
Gprin3	0.33	0.44	0.35	0.26	0.24	0.40	0.25	0.44
Gm10319	0.11	0.17	0.44	0.16	0.19	0.11	0.23	0.44
Hk2	0.36	0.39	0.27	0.44	0.21	0.40	0.23	0.44
4930590J08Rik	0.33	0.37	0.25	0.25	0.33	0.44	0.19	0.44
5430402O13Rik	0.19	0.25	0.36	0.32	0.44	0.26	0.32	0.44
Jagn1	0.18	0.23	0.44	0.18	0.21	0.31	0.19	0.44
B4galnt3	0.28	0.44	0.23	0.19	0.31	0.42	0.20	0.44
march8	0.25	0.27	0.18	0.21	0.22	0.43	0.17	0.43
Lpar5	0.27	0.37	0.25	0.25	0.33	0.43	0.30	0.43
Ggct	0.30	0.28	0.28	0.26	0.43	0.16	0.13	0.43
Gimap1	0.28	0.37	0.27	0.30	0.43	0.28	0.39	0.43
Lmod3	0.42	0.41	0.43	0.32	0.14	0.23	0.21	0.43
Foxi3	0.26	0.24	0.28	0.25	0.38	0.43	0.15	0.43
Nat8f3	0.42	0.33	0.42	0.40	0.43	0.33	0.35	0.43
Dcp1b	0.36	0.43	0.29	0.29	0.03	0.24	0.40	0.43
Vmn1r53	0.27	0.43	0.36	0.28	0.26	0.26	0.25	0.43
Fkbp14	0.37	0.42	0.28	0.33	0.28	0.43	0.21	0.43
Pradc1	0.18	0.34	0.18	0.36	0.42	0.19	0.10	0.42
Gimap3	0.33	0.38	0.39	0.37	0.42	0.37	0.42	0.42
Setmar	0.28	0.42	0.18	0.19	0.26	0.33	0.16	0.42
Reep1	0.38	0.42	0.39	0.28	0.30	0.10	0.31	0.42
Vmn1r9	0.23	0.20	0.35	0.32	0.42	0.27	0.18	0.42
Vmn1r50	0.30	0.36	0.42	0.35	0.27	0.24	0.30	0.42
Zfp746	0.21	0.42	0.23	0.21	0.16	0.26	0.21	0.42
Crbn	0.19	0.42	0.20	0.15	0.21	0.19	0.20	0.42
Xpc	0.29	0.42	0.26	0.39	0.33	0.34	0.38	0.42
Gxylt2	0.34	0.37	0.27	0.27	0.22	0.42	0.28	0.42
Trnt1	0.15	0.18	0.16	0.15	0.42	0.14	0.14	0.42
Herc6	0.33	0.41	0.33	0.29	0.40	0.42	0.29	0.42
Vmn2r25	0.24	0.25	0.35	0.26	0.16	0.42	0.22	0.42
Itprid1	0.20	0.31	0.28	0.27	0.15	0.42	0.26	0.42
Tia1	0.20	0.29	0.35	0.29	0.41	0.20	0.41	0.41

Nat8f5	0.34	0.41	0.35	0.28	0.34	0.24	0.28	0.41
Clec4b1	0.24	0.30	0.41	0.40	0.40	0.32	0.40	0.41
Kbtbd8	0.22	0.24	0.35	0.19	0.41	0.27	0.16	0.41
Mug2	0.32	0.41	0.30	0.33	0.25	0.32	0.27	0.41
Znrf2	0.34	0.41	0.25	0.16	0.32	0.27	0.29	0.41
Cpvl	0.28	0.41	0.33	0.29	0.25	0.21	0.33	0.41
Thnsl2	0.41	0.34	0.29	0.30	0.32	0.40	0.13	0.41
Bms1	0.18	0.27	0.24	0.17	0.41	0.21	0.19	0.41
C1rb	0.27	0.35	0.39	0.32	0.32	0.41	0.16	0.41
Gimap6	0.32	0.38	0.41	0.29	0.36	0.30	0.35	0.41
Hibadh	0.37	0.30	0.26	0.41	0.24	0.34	0.19	0.41
Usp39	0.17	0.41	0.26	0.18	0.38	0.18	0.17	0.41
Ccser1	0.35	0.41	0.27	0.25	0.22	0.27	0.18	0.41
Eogt	0.41	0.31	0.24	0.29	0.38	0.29	0.38	0.41
Prrt3	0.34	0.39	0.41	0.30	0.30	0.34	0.22	0.41
Ttll3	0.22	0.33	0.41	0.32	0.33	0.17	0.37	0.41
Tmem72	0.40	0.35	0.40	0.29	0.36	0.30	0.25	0.40
Sec13	0.13	0.21	0.16	0.22	0.40	0.20	0.12	0.40
Cracr2a	0.34	0.26	0.37	0.30	0.29	0.21	0.40	0.40
Chchd4	0.31	0.40	0.23	0.30	0.15	0.21	0.17	0.40
Ppm1k	0.36	0.40	0.28	0.25	0.32	0.18	0.22	0.40
Eefsec	0.15	0.40	0.20	0.16	0.15	0.34	0.14	0.40
Jazf1	0.27	0.40	0.25	0.22	0.33	0.30	0.12	0.40
Camk1	0.31	0.33	0.35	0.18	0.13	0.40	0.25	0.40
Zfand4	0.25	0.35	0.40	0.27	0.25	0.18	0.17	0.40
2310069B03Rik	0.24	0.24	0.40	0.33	0.30	0.13	0.36	0.40
Shq1	0.12	0.28	0.29	0.27	0.40	0.19	0.21	0.40
V1ra8	0.23	0.25	0.30	0.20	0.18	0.40	0.23	0.40
Rad18	0.21	0.37	0.40	0.29	0.29	0.21	0.31	0.40
Gm765	0.19	0.33	0.36	0.32	0.27	0.34	0.40	0.40
Lsm5	0.11	0.21	0.28	0.19	0.40	0.19	0.20	0.40
Pdzrn3	0.32	0.36	0.17	0.10	0.39	0.25	0.33	0.39
Tafa4	0.24	0.34	0.39	0.32	0.25	0.18	0.31	0.39
Polr1a	0.33	0.39	0.23	0.24	0.16	0.38	0.11	0.39
Vmn1r33	0.27	0.22	0.30	0.30	0.35	0.28	0.39	0.39
Paip2b	0.19	0.39	0.18	0.21	0.39	0.27	0.25	0.39
Mindy4	0.28	0.39	0.29	0.25	0.13	0.21	0.23	0.39
C130060K24Rik	0.25	0.26	0.39	0.24	0.14	0.27	0.38	0.39
Gcfc2	0.22	0.32	0.39	0.21	0.15	0.26	0.26	0.39
Doxl2	0.29	0.29	0.33	0.26	0.25	0.39	0.20	0.39
Vmn1r48	0.18	0.24	0.27	0.27	0.20	0.39	0.26	0.39
Dnah6	0.39	0.37	0.33	0.30	0.12	0.34	0.24	0.39
Slc25a26	0.28	0.39	0.29	0.28	0.24	0.20	0.27	0.39

Sh2d6	0.32	0.39	0.27	0.28	0.20	0.31	0.24	0.39
Mrpl35	0.13	0.20	0.13	0.28	0.38	0.28	0.19	0.38
Uba3	0.24	0.35	0.19	0.31	0.38	0.22	0.33	0.38
Rpn1	0.18	0.38	0.23	0.20	0.24	0.23	0.20	0.38
C1s2	0.11	0.17	0.38	0.30	0.15	0.15	0.27	0.38
Gimap8	0.29	0.29	0.27	0.31	0.35	0.27	0.38	0.38
Wdr54	0.23	0.38	0.33	0.22	0.35	0.20	0.32	0.38
Isy1	0.15	0.34	0.38	0.20	0.22	0.26	0.25	0.38
Pyurf	0.25	0.38	0.22	0.19	0.14	0.19	0.10	0.38
Cand2	0.28	0.38	0.27	0.24	0.24	0.25	0.28	0.38
Ncapd2	0.10	0.38	0.18	0.32	0.18	0.34	0.18	0.38
Zfp786	0.29	0.31	0.33	0.31	0.32	0.33	0.38	0.38
Vmn1r11	0.23	0.34	0.33	0.34	0.38	0.14	0.33	0.38
Suclg2	0.37	0.30	0.38	0.22	0.18	0.26	0.15	0.38
Tafa1	0.23	0.28	0.38	0.24	0.33	0.16	0.28	0.38
Pex26	0.25	0.38	0.20	0.28	0.21	0.37	0.18	0.38
D6Ertd527e	0.22	0.38	0.35	0.26	0.19	0.28	0.21	0.38
Vmn1r19	0.17	0.38	0.27	0.21	0.30	0.17	0.23	0.38
Prdm5	0.37	0.37	0.28	0.31	0.35	0.25	0.31	0.37
Zfp398	0.29	0.37	0.34	0.35	0.34	0.21	0.30	0.37
Tigar	0.35	0.37	0.27	0.20	0.09	0.26	0.24	0.37
Bcl2l13	0.36	0.37	0.35	0.21	0.26	0.33	0.29	0.37
Vmn1r30	0.24	0.36	0.37	0.34	0.33	0.24	0.32	0.37
Rpl32	0.29	0.29	0.37	0.18	0.12	0.29	0.33	0.37
Vmn1r39	0.30	0.33	0.22	0.24	0.37	0.23	0.26	0.37
Dusp11	0.22	0.23	0.22	0.19	0.17	0.37	0.25	0.37
Nat8f6	0.28	0.37	0.25	0.20	0.26	0.34	0.20	0.37
Slc25a18	0.27	0.37	0.33	0.26	0.28	0.30	0.32	0.37
Il23r	0.26	0.37	0.33	0.31	0.16	0.34	0.28	0.37
Fancd2os	0.33	0.37	0.22	0.23	0.21	0.19	0.34	0.37
Gkn3	0.26	0.31	0.36	0.20	0.20	0.26	0.23	0.36
Hoxaas3	0.13	0.18	0.14	0.21	0.20	0.17	0.36	0.36
Lpcat3	0.25	0.29	0.24	0.28	0.21	0.36	0.12	0.36
1600015I10Rik	0.33	0.29	0.32	0.29	0.21	0.36	0.32	0.36
Vmn1r43	0.29	0.24	0.27	0.27	0.36	0.16	0.30	0.36
Pcyox1	0.31	0.36	0.34	0.17	0.35	0.15	0.22	0.36
Zfp248	0.31	0.36	0.33	0.28	0.19	0.34	0.29	0.36
Vmn1r5	0.22	0.21	0.31	0.32	0.20	0.10	0.36	0.36
Kbtbd2	0.21	0.36	0.24	0.22	0.17	0.23	0.19	0.36
Vmn1r8	0.24	0.22	0.29	0.29	0.36	0.14	0.25	0.36
Hmces	0.25	0.36	0.18	0.21	0.18	0.26	0.19	0.36
Clec4a1	0.27	0.30	0.36	0.32	0.30	0.31	0.22	0.36
Herc3	0.25	0.31	0.23	0.23	0.26	0.36	0.17	0.36

Rpusd3	0.25	0.36	0.28	0.21	0.22	0.12	0.31	0.36
Ccdc174	0.26	0.31	0.22	0.18	0.18	0.36	0.20	0.36
Tex37	0.25	0.27	0.36	0.31	0.33	0.17	0.27	0.36
Lrrtm4	0.26	0.28	0.36	0.27	0.28	0.31	0.31	0.36
0610030E20Rik	0.19	0.35	0.36	0.28	0.18	0.35	0.26	0.36
Tprkb	0.17	0.27	0.35	0.27	0.16	0.33	0.24	0.35
Zfp282	0.14	0.35	0.26	0.23	0.23	0.18	0.18	0.35
Mat2a	0.24	0.31	0.35	0.19	0.13	0.25	0.19	0.35
Cdca3	0.20	0.32	0.34	0.20	0.35	0.35	0.20	0.35
Stk31	0.35	0.25	0.34	0.34	0.31	0.15	0.32	0.35
Vmn2r24	0.22	0.19	0.30	0.30	0.18	0.26	0.35	0.35
C87436	0.22	0.35	0.25	0.28	0.16	0.25	0.19	0.35
Nagk	0.27	0.32	0.24	0.18	0.13	0.35	0.16	0.35
Olfr214	0.22	0.21	0.35	0.31	0.21	0.24	0.31	0.35
Vmn1r38	0.18	0.35	0.24	0.26	0.23	0.26	0.32	0.35
Phb2	0.21	0.35	0.18	0.24	0.25	0.09	0.14	0.35
Vmn1r23	0.24	0.21	0.31	0.26	0.26	0.28	0.35	0.35
Rnu7	0.18	0.35	0.18	0.15	0.22	0.17	0.30	0.35
Rpia	0.13	0.34	0.30	0.28	0.24	0.21	0.16	0.34
Vmn1r54	0.24	0.25	0.28	0.29	0.34	0.17	0.32	0.34
Mkrn2os	0.32	0.30	0.28	0.24	0.15	0.34	0.15	0.34
Malsu1	0.15	0.23	0.34	0.19	0.18	0.24	0.18	0.34
Vmn2r27	0.21	0.28	0.22	0.20	0.29	0.34	0.20	0.34
Tatdn2	0.28	0.34	0.27	0.21	0.12	0.34	0.31	0.34
Rny3	0.22	0.21	0.20	0.20	0.20	0.34	0.30	0.34
Ssu2	0.31	0.32	0.34	0.30	0.25	0.32	0.29	0.34
Vmn2r20	0.21	0.29	0.28	0.34	0.18	0.17	0.27	0.34
Vmn1r21	0.23	0.28	0.26	0.17	0.15	0.34	0.19	0.34
Vmn1r32	0.06	0.20	0.34	0.25	0.24	0.21	0.21	0.34
Zfp638	0.18	0.22	0.29	0.21	0.21	0.14	0.34	0.34
Ccdc77	0.14	0.24	0.29	0.25	0.34	0.17	0.17	0.34
Vmn1r37	0.27	0.33	0.30	0.25	0.23	0.26	0.32	0.33
Olfr213	0.24	0.28	0.28	0.29	0.13	0.33	0.29	0.33
Vmn2r23	0.21	0.20	0.22	0.26	0.24	0.33	0.12	0.33
Vmn2r19	0.26	0.24	0.30	0.27	0.33	0.31	0.24	0.33
Snrnp27	0.14	0.33	0.18	0.18	0.26	0.22	0.21	0.33
Tamm41	0.10	0.21	0.30	0.21	0.33	0.18	0.19	0.33
Vmn2r21	0.17	0.26	0.29	0.33	0.20	0.16	0.24	0.33
Ruvbl1	0.18	0.30	0.21	0.21	0.33	0.20	0.21	0.33
4933431G14Rik	0.24	0.24	0.33	0.25	0.29	0.16	0.24	0.33
Vmn1r28	0.17	0.29	0.20	0.29	0.33	0.19	0.14	0.33
Rad51ap1	0.17	0.33	0.24	0.29	0.27	0.06	0.29	0.33
1700054K19Rik	0.17	0.15	0.33	0.28	0.19	0.11	0.22	0.33

Rny1	0.24	0.21	0.12	0.16	0.28	0.33	0.13	0.33
Dyrk4	0.26	0.32	0.26	0.25	0.22	0.23	0.30	0.32
Nt5c3	0.23	0.32	0.24	0.17	0.23	0.16	0.20	0.32
Gm9871	0.17	0.16	0.32	0.28	0.30	0.06	0.19	0.32
Hnrnpf	0.18	0.32	0.21	0.18	0.27	0.28	0.19	0.32
Mrpl19	0.14	0.22	0.32	0.24	0.29	0.18	0.18	0.32
Efcab12	0.30	0.29	0.32	0.21	0.13	0.09	0.21	0.32
Rbsn	0.23	0.32	0.28	0.15	0.18	0.20	0.21	0.32
Thumpd3	0.17	0.32	0.17	0.26	0.22	0.22	0.14	0.32
Grcc10	0.30	0.31	0.27	0.21	0.22	0.20	0.24	0.31
Clec4b2	0.28	0.27	0.18	0.28	0.25	0.24	0.31	0.31
Zfp422	0.17	0.24	0.20	0.26	0.31	0.19	0.15	0.31
Vmn1r22	0.22	0.31	0.28	0.27	0.13	0.25	0.28	0.31
Chmp3	0.15	0.31	0.26	0.19	0.12	0.27	0.20	0.31
4930417O13Rik	0.24	0.15	0.15	0.28	0.07	0.31	0.19	0.31
Zfp637	0.18	0.30	0.18	0.18	0.17	0.31	0.16	0.31
Vmn1r35	0.25	0.25	0.31	0.30	0.13	0.22	0.14	0.31
Suclg1	0.22	0.23	0.17	0.31	0.18	0.09	0.19	0.31
Vmn1r6	0.23	0.21	0.28	0.26	0.18	0.23	0.31	0.31
2610300M13Rik	0.11	0.24	0.30	0.19	0.21	0.11	0.19	0.30
Plekha8	0.25	0.30	0.24	0.23	0.19	0.30	0.19	0.30
Zfp862-ps	0.22	0.30	0.12	0.21	0.25	0.13	0.16	0.30
Svs1	0.24	0.30	0.25	0.25	0.22	0.23	0.22	0.30
1700069P05Rik	0.17	0.23	0.25	0.28	0.30	0.16	0.25	0.30
Vmn1r51	0.30	0.27	0.22	0.23	0.14	0.27	0.24	0.30
D6Wsu163e	0.19	0.30	0.28	0.16	0.21	0.24	0.18	0.30
6330415B21Rik	0.22	0.24	0.24	0.28	0.24	0.21	0.30	0.30
Vmn1r4	0.23	0.24	0.30	0.19	0.19	0.19	0.26	0.30
Zfp775	0.25	0.30	0.20	0.23	0.17	0.23	0.18	0.30
Tsen2	0.29	0.24	0.24	0.14	0.17	0.28	0.09	0.29
Mogs	0.19	0.29	0.17	0.17	0.13	0.12	0.16	0.29
Tnip3	0.21	0.29	0.26	0.28	0.19	0.22	0.23	0.29
Olfr211	0.19	0.24	0.26	0.29	0.17	0.22	0.23	0.29
Vmn1r34	0.19	0.24	0.28	0.22	0.26	0.26	0.14	0.28
Vmn1r16	0.19	0.15	0.23	0.26	0.22	0.21	0.28	0.28
9530062K07Rik	0.24	0.22	0.28	0.12	0.19	0.21	0.23	0.28
Vmn1r36	0.24	0.25	0.28	0.22	0.18	0.18	0.24	0.28
Ndufa9	0.22	0.23	0.16	0.28	0.14	0.18	0.19	0.28
1700026J14Rik	0.16	0.20	0.19	0.13	0.15	0.28	0.20	0.28
Snrpg	0.18	0.21	0.17	0.25	0.28	0.16	0.15	0.28
Clec4a4	0.17	0.14	0.28	0.20	0.22	0.23	0.25	0.28
Vmn1r24	0.28	0.26	0.26	0.21	0.18	0.15	0.24	0.28
1700030F04Rik	0.13	0.20	0.27	0.16	0.10	0.25	0.27	0.27

Vmn1r52	0.23	0.27	0.16	0.25	0.19	0.26	0.26	0.27
2610306M01Rik	0.16	0.27	0.26	0.23	0.26	0.10	0.15	0.27
Zfp212	0.19	0.25	0.27	0.25	0.16	0.18	0.22	0.27
Vmn2r22	0.16	0.22	0.22	0.27	0.18	0.14	0.25	0.27
Ccdc126	0.20	0.27	0.25	0.21	0.18	0.20	0.21	0.27
Vmn1r17	0.16	0.24	0.25	0.24	0.17	0.24	0.26	0.26
Rnf181	0.21	0.24	0.21	0.21	0.14	0.26	0.19	0.26
Vmn1r31	0.18	0.26	0.26	0.23	0.15	0.21	0.22	0.26
1700065L07Rik	0.10	0.25	0.17	0.21	0.11	0.16	0.19	0.25
Vmn1r18	0.19	0.16	0.23	0.22	0.20	0.24	0.15	0.24
Tigd2	0.22	0.22	0.17	0.21	0.18	0.24	0.20	0.24
Nfu1	0.17	0.22	0.16	0.19	0.23	0.12	0.20	0.23
Rprl1	0.22	0.12	0.18	0.14	0.23	0.14	0.12	0.23
1700049E22Rik	0.16	0.22	0.17	0.14	0.10	0.17	0.10	0.22
1700094M24Rik	0.20	0.17	0.22	0.13	0.11	0.11	0.09	0.22
Emc3	0.18	0.21	0.16	0.16	0.18	0.20	0.17	0.21
1700124L16Rik	0.13	0.13	0.15	0.20	0.05	0.08	0.19	0.20
Rpl34-ps1	0.14	0.15	0.07	0.14	0.16	0.09	0.13	0.16

Genes are ranked according to the maximum individual score from any phenotype module. PTX, pertussis toxin; T1H, Type 1 hypersensitivity; VP, vascular permeability; GPCR, G-protein coupled receptor, ER, endoplasmic reticulum. EMC, endoplasmic membrane protein complex; ERAD, endoplasmic reticulum-associated degradation.

Supplementary Table 5. Details of primers used in this study.

Microsatellite primers

Name	Mbp	Forward	Reverse
D6Mit17	71.06	5’-ggcttgccaacaaaactgat-3’	5’-gggttttccccttcaaatgt-3’
D6Mit8	83.66	5’-tgcacagcagctcattctct-3’	5’-ggaaggaaggagtggggtag-3’
D6Mit65	101.33	5’-ctccgcaaacatgtgtatatgt-3’	5’-ggactcaaacttgctcactgg-3’
D6Mit149	105.95	5’-acatgcatgcacaactccat-3’	5’-ttttttgtgggctgcatgta-3’
D6Mit105	107.74	5’-ctgctccactacttctattcctgg-3’	5’-caaagccttatatattacacctcacc-3’
D6Mit115	116.61	5’-ccatttaataagtgatccctctgg-3’	5’-tgtcacaccacaatgggc-3’
D6Mit254	125.30	5’-agtgtccctaggggtgg-3’	5’-ggggccttagaggtagcaac-3’

Sequence-specific primers

Name	Mbp	Forward1	Forward2	Reverse
rs36743061	81.89	5’-ctgcagagatgactaacttccacac-3’	5’-ctgcagagatgactaacttccacaa-3’	5’-gacggggcagcaaatcttat-3’
rs30936839	89.22	5’-tttatggagagcagcatggag-3’	5’-tttatggagagcagcatggac-3’	5’-tactgctgtggacagccaac-3’
rs29868697	108.45	5’-ccacactggtcaggcctc-3’	5’-ccacactggtcaggcctt-3’	5’-attgaaagctcccagcagaa-3’
rs6257334	119.91	5’-agttgcttctgttctcattgctatg-3’	5’-agttgcttctgttctcattgctatt-3’	5’-tctagctggggtgcattacc-3’

***Hrh1* primers**

Name	Mbp	Forward	Reverse
Hrh1 WT	114.30	5’-tgaagtatctggctctgagtgg-3’	5’-ccatccgatggctccctccctgggag-3’
Hrh1 KO	114.30	5’-tgaagtatctggctctgagtgg-3’	5’-tctatcgccttcttgaccgag-3’

Supplementary Table 6. List of datasets retrieved from mouse phenome database (www.phenome.jax.org) to collate SNP information across all studied mouse strains [41, 42, 66-71].

Data set	Procedure	What's in this data set	Panel	Sex	Year
Broad2	genotyping	SNP profiling, 131,000+ genomic locations, 1-19,X.	inbred		2009
CGD-MDA1	genotyping	SNP profiling, 470,000+ genomic locations, 1-19,X,Y,MT.	inbred	m	2014
CGD-MDA2	genotyping	SNP profiling, 470,000+ genomic locations, 1-19,X,Y,MT.	BXD w/par	m	2014
CGD-MDA3	genotyping	SNP profiling, 470,000+ genomic locations, 1-19,X,Y,MT.	ILSXISS w/par	m	2014
CGD-MDA4	genotyping	SNP profiling, 470,000+ genomic locations, 1-19,X,Y,MT.	AXB, BXA, BXH, CXB, AKXL w/par	m	2014
CGD-MDA5	genotyping	SNP profiling, 470,000+ genomic locations, 1-19,X,Y,MT.	B6.A, B6.PWD consomic panels	m	2014
Perlegen2	genotyping	SNP profiling, 8,100,000+ genomic locations, 1-19,X,Y,MT.	inbred	m	2005
Sanger4	genotyping	SNP profiling, 80,000,000+ genomic locations. SNPs and indels. 1-19,X.	inbred	both	2017
UCLA1	genotyping	SNP profiling, 132,000+ genomic locations, 1-19,X	HMDP	both	2018
UNC-GMUGA1	genotyping	SNP profiling, 130,000+ genomic locations, 1-19,X,Y,MT.	CC w/par	m	2020
UNC-MMUGA2	genotyping	SNP profiling, 76,000+ genomic locations, 1-19,X,MT	CC w/par	both	2017

Supplementary Figure 1. Mouse family tree (adapted from Petkov *et al*. [22]) showing the phylogenetic relationships among 102 inbred and wild-derived inbred strains. Group 1, Bagg albino derivatives; Group 2, Swiss mice; Group 3, Japanese and New Zealand inbred strains; Group 4, C57/58 strains; Group 5, Castle mice; Group 6, C.C. Little DBA and related strains; Group 7, wild-derived strains. Strains with *Hrh1*^{r} allele are highlighted and their Bphs susceptibility color coded. Red = Bphs^{s}, Green = Bphs^{r}, and Black = Bphs unknown (Bphs$^{?}$).

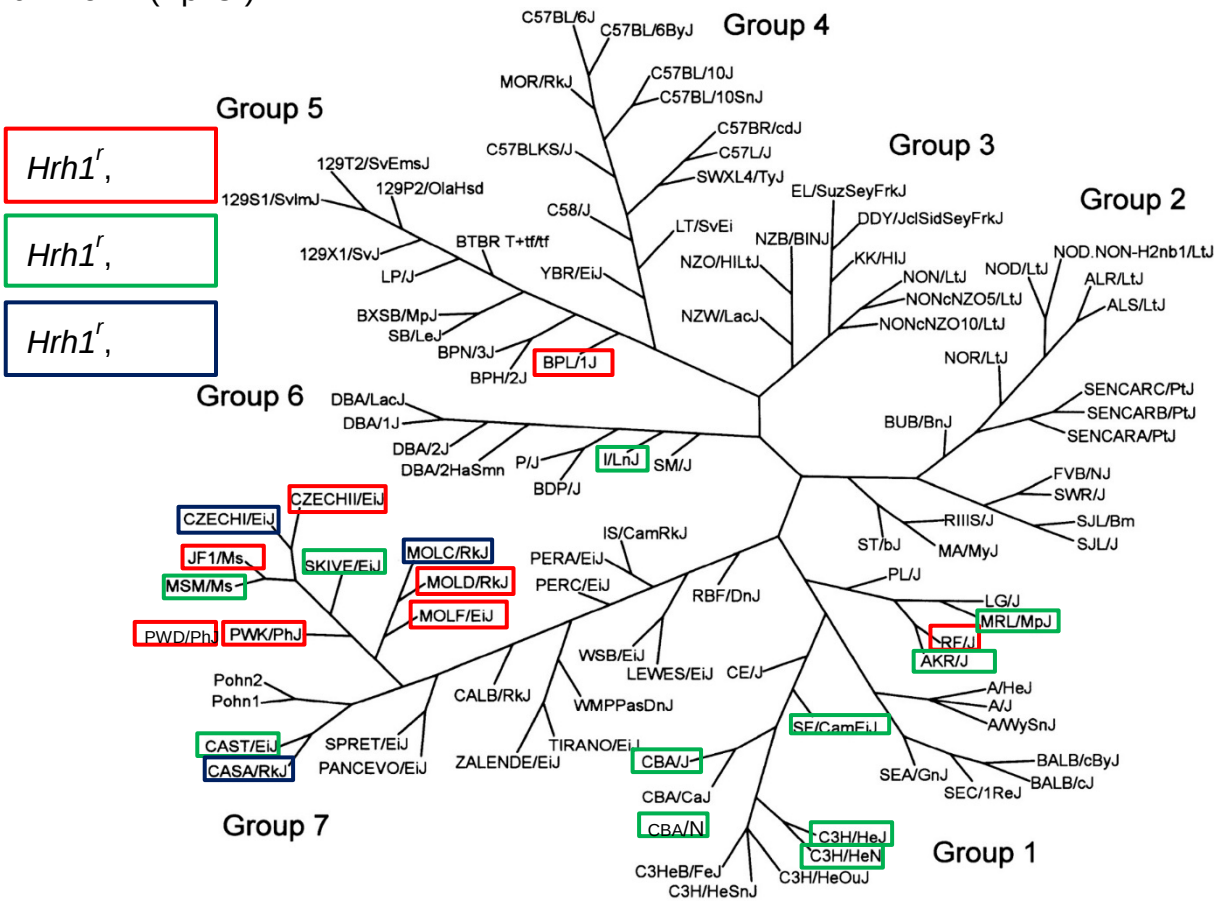

Supplementary Figure 2. The predicted candidates for *Bphse* overlaps with *Bphs/Hrh1*, *Histh3,* and *Histh4* in agreement with the genetic data that a functional LD on Chr6 encodes genes that control both *B. pertussis*/PTX-dependent and age- and inflammation-dependent susceptibility to HA-shock.